ISSN 1007-9327 (print)
ISSN 2219-2840 (online)

World Journal of *Gastroenterology*

World J Gastroenterol 2022 July 14; 28(26): 3008-3281

Published by Baishideng Publishing Group Inc

World Journal of Gastroenterology

Contents

Weekly Volume 28 Number 26 July 14, 2022

REVIEW

MINIREVIEWS

ORIGINAL ARTICLE

Basic Study

World Journal of Gastroenterology

Weekly Volume 28 Number 26 July 14, 2022

Contents

Contents

ABOUT COVER

Editorial Board Member of *World Journal of Gastroenterology*, Koichi Suda, MD, PhD, FACS, Professor and Head, Divisions of GI and HPB Surgery, Department of Surgery, Fujita Health University, Rm C908, 1-98 Dengakugakubo, Kutsukake, Toyoake, Aichi 470-1192, Japan. ko-suda@fujita-hu.ac.jp

AIMS AND SCOPE

The primary aim of *World Journal of Gastroenterology* (*WJG*, *World J Gastroenterol*) is to provide scholars and readers from various fields of gastroenterology and hepatology with a platform to publish high-quality basic and clinical research articles and communicate their research findings online. *WJG* mainly publishes articles reporting research results and findings obtained in the field of gastroenterology and hepatology and covering a wide range of topics including gastroenterology, hepatology, gastrointestinal endoscopy, gastrointestinal surgery, gastrointestinal oncology, and pediatric gastroenterology.

INDEXING/ABSTRACTING

The *WJG* is now abstracted and indexed in Science Citation Index Expanded (SCIE, also known as SciSearch®), Current Contents/Clinical Medicine, Journal Citation Reports, Index Medicus, MEDLINE, PubMed, PubMed Central, Scopus, Reference Citation Analysis, China National Knowledge Infrastructure, China Science and Technology Journal Database, and Superstar Journals Database. The 2022 edition of Journal Citation Reports® cites the 2021 impact factor (IF) for *WJG* as 5.374; IF without journal self cites: 5.187; 5-year IF: 5.715; Journal Citation Indicator: 0.84; Ranking: 31 among 93 journals in gastroenterology and hepatology; and Quartile category: Q2. The *WJG*'s CiteScore for 2021 is 8.1 and Scopus CiteScore rank 2021: Gastroenterology is 18/149.

RESPONSIBLE EDITORS FOR THIS ISSUE

Production Editor: *Hua-Ge Yu*; **Production Department Director:** *Xu Guo*; **Editorial Office Director:** *Jia-Ru Fan*.

NAME OF JOURNAL
World Journal of Gastroenterology

ISSN
ISSN 1007-9327 (print) ISSN 2219-2840 (online)

LAUNCH DATE
October 1, 1995

FREQUENCY
Weekly

EDITORS-IN-CHIEF
Andrzej S Tarnawski

EDITORIAL BOARD MEMBERS
http://www.wjgnet.com/1007-9327/editorialboard.htm

PUBLICATION DATE
July 14, 2022

INSTRUCTIONS TO AUTHORS
https://www.wjgnet.com/bpg/gerinfo/204

GUIDELINES FOR ETHICS DOCUMENTS
https://www.wjgnet.com/bpg/GerInfo/287

GUIDELINES FOR NON-NATIVE SPEAKERS OF ENGLISH
https://www.wjgnet.com/bpg/gerinfo/240

PUBLICATION ETHICS
https://www.wjgnet.com/bpg/GerInfo/288

PUBLICATION MISCONDUCT
https://www.wjgnet.com/bpg/gerinfo/208

ARTICLE PROCESSING CHARGE
https://www.wjgnet.com/bpg/gerinfo/242

STEPS FOR SUBMITTING MANUSCRIPTS
https://www.wjgnet.com/bpg/GerInfo/239

ONLINE SUBMISSION
https://www.f6publishing.com

World Journal of Gastroenterology

Submit a Manuscript: https://www.f6publishing.com

World J Gastroenterol 2022 July 14; 28(26): 3008-3026

DOI: 10.3748/wjg.v28.i26.3008

ISSN 1007-9327 (print) ISSN 2219-2840 (online)

REVIEW

Advances in the imaging of gastroenteropancreatic neuroendocrine neoplasms

Anupama Ramachandran, Kumble Seetharama Madhusudhan

Specialty type: Radiology, nuclear medicine and medical imaging

Provenance and peer review: Invited article; Externally peer reviewed.

Peer-review model: Single blind

Peer-review report's scientific quality classification

Grade A (Excellent): A
Grade B (Very good): B
Grade C (Good): C, C
Grade D (Fair): 0
Grade E (Poor): 0

P-Reviewer: Cerwenka H, Austria; Wang WQ, China

Received: October 11, 2021
Peer-review started: October 11, 2021
First decision: November 15, 2021
Revised: November 30, 2021
Accepted: June 19, 2022
Article in press: June 19, 2022
Published online: July 14, 2022

Anupama Ramachandran, Kumble Seetharama Madhusudhan, Department of Radiodiagnosis and Interventional Radiology, All India Institute of Medical Sciences, New Delhi 110029, India

Corresponding author: Kumble Seetharama Madhusudhan, MD, Additional Professor, Department of Radiodiagnosis and Interventional Radiology, All India Institute of Medical Sciences, Ansari Nagar, New Delhi 110029, India. drmadhuks@gmail.com

Abstract

Gastroenteropancreatic neuroendocrine neoplasms comprise a heterogeneous group of tumors that differ in their pathogenesis, hormonal syndromes produced, biological behavior and consequently, in their requirement for and/or response to specific chemotherapeutic agents and molecular targeted therapies. Various imaging techniques are available for functional and morphological evaluation of these neoplasms and the selection of investigations performed in each patient should be customized to the clinical question. Also, with the increased availability of cross sectional imaging, these neoplasms are increasingly being detected incidentally in routine radiology practice. This article is a review of the various imaging modalities currently used in the evaluation of neuroendocrine neoplasms, along with a discussion of the role of advanced imaging techniques and a glimpse into the newer imaging horizons, mostly in the research stage.

Key Words: Neuroendocrine tumor; Gastroenteropancreatic; Intravoxel incoherent motion; Diffusion weighted imaging; Perfusion imaging; Dual energy computed tomography

Core Tip: The prognosis of gastroenteropancreatic neuroendocrine neoplasms (GEPNENs) depends on the stage of the disease and tumor grade. Traditional imaging techniques like multiphase contrast-enhanced computed tomography perform well at disease staging. For tumor grading, histopathological examination, with determination of number of mitoses and Ki-67 index is considered optimal. Advances in imaging techniques have enabled detection of smaller neuroendocrine neoplasms (< 2 cm). By analysing functional information like diffusion, perfusion and tumor heterogeneity, quantitative imaging is currently focused on noninvasive prediction of the grade of GEPNENs preoperatively.

Citation: Ramachandran A, Madhusudhan KS. Advances in the imaging of gastroenteropancreatic neuroendocrine neoplasms. *World J Gastroenterol* 2022; 28(26): 3008-3026
URL: https://www.wjgnet.com/1007-9327/full/v28/i26/3008.htm
DOI: https://dx.doi.org/10.3748/wjg.v28.i26.3008

INTRODUCTION

Gastroenteropancreatic neuroendocrine neoplasms (GEPNENs) are a rare and heterogeneous group of tumors that originate from the gastrointestinal and pancreatic neuroendocrine cells[1,2]. They may be benign or malignant and may or may not secrete hormones. Use of the previous terminology - carcinoid tumor - is no longer encouraged. The gastrointestinal tract (GIT), having the highest density of neuroendocrine cells in the body, is the most common site of involvement of neuroendocrine neoplasms (NENs), comprising nearly 60% of all NENs[3]. Pancreatic NENs (PNENs) account for about 7% of all GEPNENs [4]. Most PNENs are sporadic. However, association with four familial syndromes (in up to 25%) is well described: multiple endocrine neoplasia type I, von Hippel Lindau syndrome, neurofibromatosis type I and tuberous sclerosis[5,6].

Classification based on histological differentiation and grade is desirable as it provides insight into tumor biology, clinical course and helps in planning management. In 2019, the 5th edition of the World Health Organization (WHO) classification of tumors series published the latest NEN classification (Table 1)[7]. The latest WHO classification recognizes that well-differentiated NENs may be high grade, but they are distinct from the poorly differentiated neuroendocrine carcinomas (NECs). Most GEPNENs are well-differentiated and slowly growing. Grade 3 NENs are most common in the pancreas, but can occur throughout the GIT[7]. Given the differences in prognosis, tumor grade is the most important factor determining the treatment of GEPNENs. The treatment of GEPNENs depends on grade, differentiation, site of origin, and stage of tumor, and the opinion about the best treatment strategy is evolving. Surgical resection remains the cornerstone and is the only curative treatment. For patients with small (< 2 cm), low-grade NENs, decisions on surgery *vs* active surveillance need to be individualized based on tumor size, morphology (homogeneous, well circumscribed tumor < 1 cm correlate with low malignant potential) and patient characteristics like age and presence of comorbidities[8].

The commonly used imaging modalities include ultrasonography (US), computed tomography (CT), magnetic resonance imaging (MRI) and positron emission tomography (PET)-CT. Imaging is primarily aimed at accurate detection, characterization and staging of these neoplasms and also at assessment of response to treatment. Sensitivity of common imaging modalities used in the evaluation of GEPNENs are summarized in Table 2.

Improvements and advances in the imaging techniques have mainly focused on the noninvasive prediction of the grade of the NENs. The European Neuroendocrine Tumor Society (ENETS) has also recommended that preoperative assessment of the grade of the NENs is essential for prognosis prediction and management planning[9]. In addition, with the improvements in the imaging technologies, the detection rates of small NENs have significantly improved, with many often being detected incidentally.

US

Transabdominal ultrasonography (USG) often is the commonest initial modality used for patients with gastrointestinal symptoms. It has value in the detection of liver metastases (sensitivity reaching 85%-90%). PNENs in general appear as hypoechoic masses with a hyperechoic halo on USG[10].

However, transabdominal USG has limitations. It has a poor sensitivity (13%-27%) for the detection of GEPNENs[11]. The technique is dependent on the experience of the operator. Presence of bowel gas and increased subcutaneous fat can obscure adequate visualization.

The advent of harmonic imaging, pulse inversion sequence, low mechanical index techniques and ultrasound contrast agents (UCAs) has enabled routine application of contrast-enhanced ultrasound (CEUS) to overcome the limitations of conventional B mode USG. The inherent advantage of CEUS is its ability to assess tumor-enhancement patterns in real time during transabdominal USG[12]. The enhancement patterns are described during arterial, portal venous and late phases. UCAs are gas microbubbles stabilized by a shell, the composition of which varies depending on the type of contrast agent. UCAs are blood pool agents and increase the back scatter of US, enhancing the echogenicity of flowing blood[12]. Harmonic imaging detects harmonic signals from the microbubbles and CEUS specific US modes filter signals from the background tissue, thereby showing even very slow blood flow without Doppler related artifacts. UCAs, unlike CT and MRI contrast agents, are excreted by the lungs and hence can be used safely in patients with deranged renal function.

Table 1 World Health Organization Classification and grading criteria for neuroendocrine neoplasms of the gastrointestinal tract and hepatopancreatobiliary organs (7)

Terminology	Differentiation	Grade	Mitoses/2 mm^2	Ki-67 index
NEN grade 1	Well differentiated	Low	< 2	< 3%
NEN grade 2		Intermediate	2-20	3%-20%
NEN grade 3		High	> 20	> 20%
SCNEC	Poorly differentiated	High[1]	> 20	> 20%
LCNEC			> 20	> 20%
MiNEN	Well or poorly differentiated	Variable	Variable	Variable

[1]Poorly differentiated neuroendocrine carcinomas are not formally graded, but are considered high-grade by definition.
LCNEC: Large cell neuroendocrine carcinoma; MiNEN: Mixed neuroendocrine non-neuroendocrine neoplasm; NEN: Neuroendocrine neoplasm; SCNEC: Small-cell neuroendocrine carcinoma.

Table 2 Sensitivity of common imaging modalities used in the evaluation of gastroenteropancreatic neuroendocrine neoplasms

Imaging modality	Sensitivity
Transabdominal USG	13%-27% for GEPNEN
Contrast enhanced ultrasound	99% in detecting liver metastases
Endoscopic ultrasonography	82%-93% for PNEN
CECT	63%-82% for PNEN
CE MRI	79% for PNEN
DWI	83% for liver metastases

USG: Ultrasonography; GEPNEN: Gastroenteropancreatic neuroendocrine neoplasms; CECT: Contrast enhanced computed tomography; CE MRI: Contrast-enhanced magnetic resonance imaging; DWI: Diffusion-weighted imaging.

The differential perfusion on CEUS has been shown to identify and diagnose pancreatic tumors. Pancreatic adenocarcinomas are in general hypovascular, while NENs are hypervascular. Takeda *et al* [13] found three patterns of hyperenhancement of PNENs and found that CEUS was useful in the differentiation of PNENs from pancreatic adenocarcinomas. Malagò *et al*[14] also showed that the enhancement patterns of nonfunctioning PNENs on CEUS (hyper-, iso- or hypovascular) correlated well with Ki-67 index and CEUS improved the detection of hepatic metastases. Hypervascular lesions had lower Ki-67 index. Another study showed that the enhancement patterns of NENs on CEUS correlated significantly with CT enhancement pattern and histological Ki-67 index and CEUS was a good predictor of response of tumors to somatostatin analogues[15].

Elastography

Elastography is an advancement in USG that enables real-time measurement of tissue stiffness along with display in colors superimposed on the grey scale images[16]. In general, elastography helps with the differentiation of benign and malignant lesions based on stiffness, as malignant lesions are usually hard. Only a few studies have reported the usefulness of transabdominal shear wave elastography (SWE) in the evaluation of pancreatic tumors. Park *et al*[17] showed that elastography can differentiate benign and malignant solid pancreatic lesions based on the difference in the shear wave velocity values (relative stiffness) between the tumor and the normal parenchyma. An early study by Uchida *et al*[18] found that NENs were homogeneous and soft on elastography, comparable to the normal pancreas. They also reported that a combination of elastography and B mode USG, improved the diagnostic accuracy to 90%, from 70%-80 % when B mode USG was used alone. However, if the visualization on the baseline B mode USG is suboptimal, the results of CEUS and elastography are also often unsatisfactory. These limitations have been overcome by the use of endoscopic ultrasound (EUS).

EUS

EUS is considered the most accurate test for the diagnosis of pancreatic masses[19]. EUS uses higher frequency (7.5-12 MHz) probes, placed in proximity to the area of interest and hence performs better at detection of tumors < 2 cm for which CT and MRI have poor sensitivity[20]. Overall, EUS has a sensitivity of 82%-93% and a specificity of 92%-95% for localizing PNENs. EUS is particularly useful in the detection of benign insulinomas that lack somatostatin receptors and consequently are not detected on somatostatin receptor scintigraphy/single photon emission computed tomography (SPECT)/PET [21]. EUS also plays an important role in the detection of functional pancreatic and extrapancreatic (duodenal) gastrinomas[22]; both of which generally have a small size (average 1 cm) at diagnosis. The additional benefit of EUS is its ability to guide accurate tissue sampling *via* fine needle aspiration and core biopsy[23]. CEUS can also be performed through EUS with the use of second generation UCAs (*e.g*, Sonovue), which produce harmonic signals at low acoustic powers. A recent study showed that the time intensity curve analysis during CEUS showed high diagnostic accuracy in grading PNENs, and could differentiate grade 1/2 tumors from grade 3 tumors/carcinomas[24].

EUS elastography

EUS elastography of the pancreas has been shown to be a promising imaging technique in several studies[25-27]. However, a prospective study by Hirche *et al*[28] including 70 patients with undifferentiated pancreatic masses showed an overall lower sensitivity (41%), specificity (53%) and accuracy (45%) for the detection of malignancy. One of the early studies evaluating conventional strain elastography for pancreatic lesions showed significant strain difference between benign and malignant masses[29]. The major utility of EUS elastography is in increasing the yield of sampling by aiding better tumor targeting, especially in the background of pancreatic parenchymal fibrosis[30]. SWE EUS is a recent development and studies evaluating its utility in the pancreas are just emerging[31,32]. A recent comparative study suggested that conventional strain elastography was superior to SWE in the characterization of pancreatic lesions[33].

CT

CT is the cornerstone and the most commonly performed imaging modality for the diagnosis and preoperative staging of GEPNEN. Standard CT scan has low sensitivity (~60%) for the detection of GIT NENs[34]. Dynamic dual-phase protocol, which includes the arterial and portal venous phases, is recommended in patients with suspected NEN[35,36] (Figure 1). For PNEN, the late arterial phase acquired at 40-45 s (pancreatic phase) suits best. For detection of small bowel NENs, CT enterography (oral administration of neutral contrast agent like mannitol for bowel distension) or CT enteroclysis (administration of neutral contrast *via* nasojejunal tube) is required. CT enteroclysis combines the advantages of enteroclysis with imaging capabilities of multidetector computed tomography (MDCT). Study by Kamaoui *et al*[37] showed that CT enteroclysis had 100% sensitivity and 96.2% specificity for the detection of small bowel NEN. A comparative study from Mayo Clinic found that CT enterography was better than capsule endoscopy in detecting small bowel tumors, with a sensitivity of up to 93%[38]. This ability of CT enterography to detect small bowel tumors remains high (sensitivity of 88%) even in the presence of gastrointestinal bleeding[39].

The characteristic imaging feature on CT scan suggesting the diagnosis of NENs is their intense enhancement in the late arterial phase, owing to the hypervascular nature of the tumor. The arterial phase also helps in outlining the relationship of the tumor with the adjacent arteries. Using the maximum intensity projection technique, virtual angiographic images can be obtained. Volume rendering techniques applied to the arterial phase provide easily explainable images to the surgeon. Portal venous phase helps to draw the relationship of the tumor with major veins, especially the splenic vein and the superior mesenteric vein for PNENs. Dual-phase imaging is also crucial for the evaluation of hepatic metastases. The classic liver metastases from NEN, being hypervascular, are most evident on the arterial phase images. About 6%-15% of NEN liver metastases are appreciated only in the arterial phase[40,41]. However up to 16% are hypovascular and show delayed enhancement[40].

One of the early studies suggested that the size of the tumor is an important prognostic factor, with tumors < 1 cm showing lesser incidence of liver metastasis (20%–30%) compared to those with > 1 cm (> 40% risk)[42]. Studies have shown that up to 42% of PNENs may not show arterial phase hyperenhancement[43,44]. Such arterial phase hypoenhancing tumors were associated with a significantly lower 5-year survival (54%) compared to the lesions which were isoenhancing (89%) or hyperenhancing (93%) [45]. Rodallec *et al*[46] found that tumor enhancement on CT scan correlated with microvascular density (MVD) evaluated on histology and that hypoenhancing PNENs correlated with poorly differentiated tumors and a decrease in overall survival rate. These studies showed that the CT enhancement characteristics of NENs have a prognostic value. Gallotti *et al*[6] found that incidentally detected PNENs, size > 3 cm, complex enhancement pattern and, presence of calcification, vascular invasion, main pancreatic duct dilatation, and peripancreatic lymph nodes were associated with nonbenign tumors and required

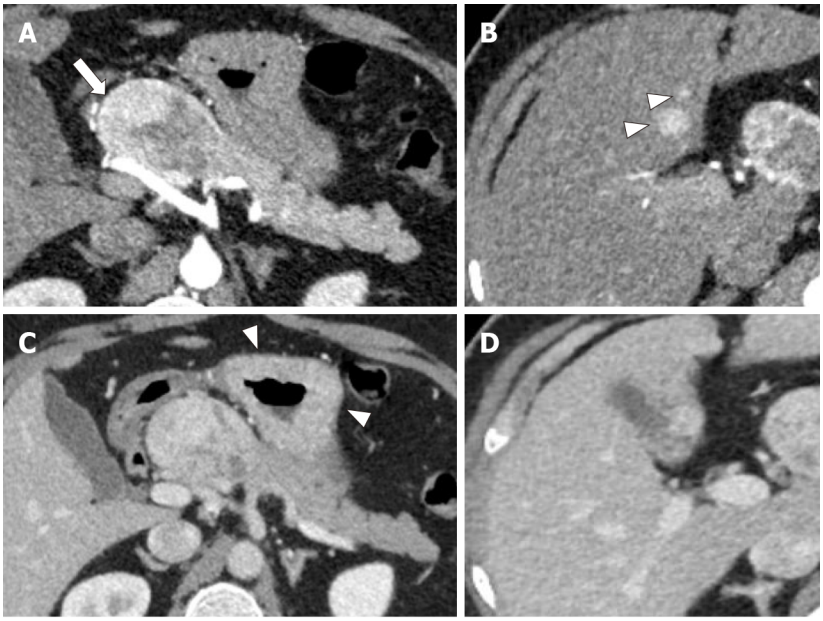

DOI: 10.3748/wjg.v28.i26.3008

Figure 1 49-year-old man with epigastric pain and raised serum gastrin levels. A and B: Axial contrast enhanced pancreatic phase computed tomography (CT) images show a well-defined hyperenhancing mass (arrow in A) in the head and neck of pancreas, abutting the proper hepatic artery along with two hyperenhancing focal lesions in the liver (arrowheads in B), indicating hepatic metastases; C and D: Axial portal venous phase CT images show retention of contrast in the lesions in both locations. Thickened gastric mucosal folds is also noted (arrowheads in C).

more aggressive course of management.

The role of various CT quantitative parameters based on enhancement of the NEN in the arterial or pancreatic and the venous phases has been evaluated in the prediction of tumor grade. Kim *et al*[47] found that portal enhancement ratio (HU value of the tumor divided by the HU value of pancreatic parenchyma on portal phase images) had the best odds ratio (49.6) and a cutoff value of < 1.1 had a sensitivity of 92% and specificity of 81% in differentiating grade 3 PNENs from grade 1 and 2. This high sensitivity and specificity of portal enhancement ratio in differentiating neuroendocrine carcinomas from well-differentiated NENs was also confirmed by another study[48]. Yamada *et al*[49] showed that corrected true enhancement values in the pancreatic phase had a sensitivity of 92%, specificity of 84% and area under the curve of 0.897 in the differentiation of grade 1 from grade 2 PNENs. D'Onofrio *et al*[50] showed that various tumor enhancement parameters (tumor permeability ratios, tumor parenchyma ratios, tumor arterial ratio and tumor venous ratio) were significantly different between grade 1 and grade 3 and between grade 2 and grade 3 PNENs. However, these values could not differentiate grade 1 from grade 2 tumors.

Dual-energy CT

Dual-energy CT (DECT) is an advancement in CT, which allows acquisition of images at two energy levels, with lower energy being 80-100 kVp and higher being 140 kVp. Using DECT, material decomposition of images and generation of iodine maps, virtual noncontrast images, and monochromatic images at different energy levels is possible (Figures 2 and 3). Monoenergetic images at low keV (55 keV) in the pancreatic phase of DECT show improved image contrast for evaluation of pancreatic masses[51]. Monochromatic spectral images improve the sensitivity of detection of NENs like insulinomas, particularly the hypovascular and isoattenuating tumors and the sensitivity is comparable to MRI[52]. One study showed that iodine uptake obtained from DECT is useful in the differentiation of hepatocellular carcinoma from liver metastases arising from NENs, with the former showing significantly higher iodine uptake (3.8 ± 1.2 *vs* 2.3 ± 0.6)[53]. This iodine uptake parameter on DECT may also be used in assessing the response to treatment of NENs.

Perfusion CT

Perfusion CT is a technique that measures the dynamic changes in the attenuation of the tissues after contrast administration. It allows quantitative measurement of tissue perfusion, thereby assisting in the assessment of tumor viability and biological behavior[54]. The commonly used quantitative parameters of perfusion CT in oncoimaging are blood flow, blood volume, vascular permeability-surface area product and mean transit time (Figures 4 and 5). These parameters serve as imaging biomarkers of tumor angiogenesis, which is ideally assessed histologically by calculating the MVD[55]. NENs are among the tumors with significant angiogenesis. Unlike majority of the cancers, where increased tumor

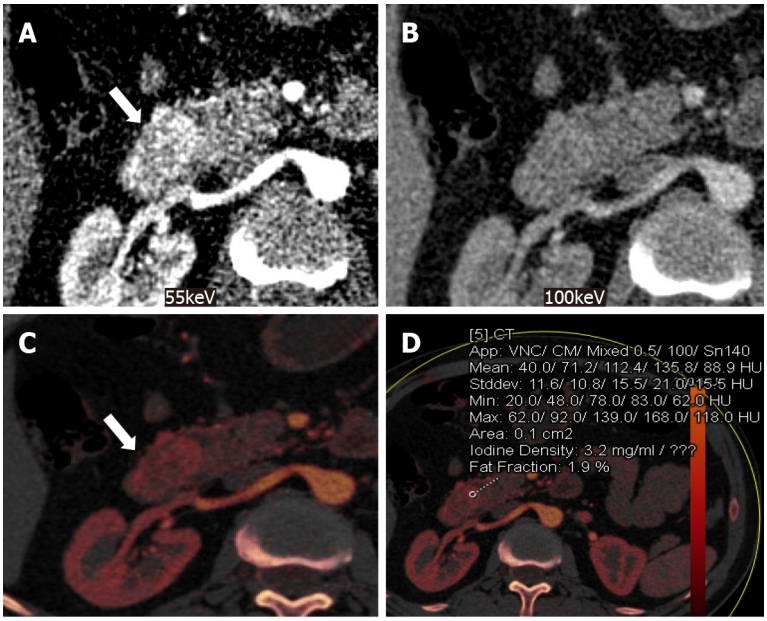

DOI: 10.3748/wjg.v28.i26.3008

Figure 2 Dual-energy computed tomography images of a 46-year-old man presenting with melena. A: Axial monochromatic computed tomography (CT) image at 55 keV in pancreatic phase shows a hyperenhancing well-defined mass (arrow) arising from the duodenal wall; B: Enhancement of the same lesion (arrow) appears subtle on the axial 100 keV monochromatic CT image; C and D: Iodine overlay maps show bright areas (arrow) suggesting contrast uptake (C), with iodine concentration of 3.2 mg/mL in areas of uptake (D). Iodine concentration of normal pancreas was 0.5 mg/mL.

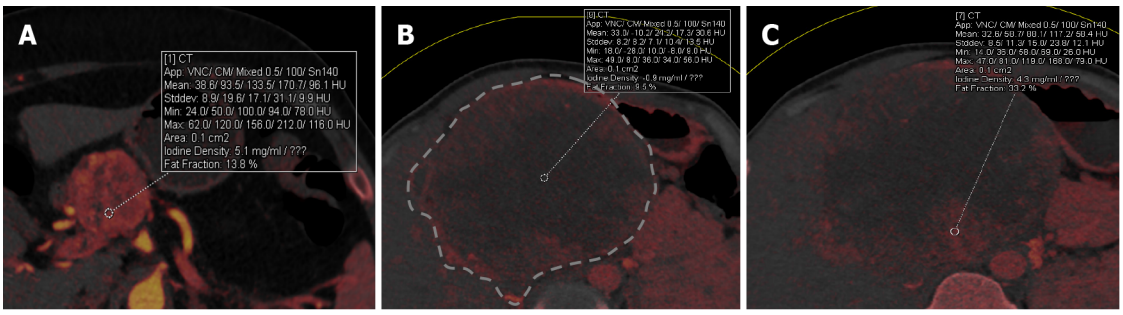

DOI: 10.3748/wjg.v28.i26.3008

Figure 3 Dual-energy computed tomography in grading the pancreatic neuroendocrine neoplasms. A: Iodine overlay dual-energy computed tomography (CT) map of a 40-year-old woman with low-grade (grade 2) pancreatic neuroendocrine neoplasms (PNEN) in head of pancreas shows hyperenhancement of the tumor with an iodine concentration of 5.1 mg/mL; B and C: Iodine overlay dual energy CT maps of a 29-year-old man with grade 3 PNEN (outlined in B) shows large hypoenhancing areas with low iodine concentration (0.9 mg/mL) and peripheral bright areas with iodine concentration of 4.3 mg/mL (C). Measuring iodine concentration helps in objectively assessing the grade of the tumor.

vascularity is associated with aggressive behavior, higher microvascular density in NENs is associated with a low tumor grade[54]. Low MVD was found to be an unfavorable prognostic factor for PNENs in several studies despite the presence of other favorable conventional histoprognostic factors, and call for a more aggressive treatment approach[56-58]. A study by d'Assignies *et al*[59] on 36 patients with PNENs found a significant correlation between MVD and blood flow assessed by using perfusion CT. In their study, the authors found that tumors that are small (< 2 cm), benign (grade 1), with a proliferation index of ≤ 2%, and without histological signs of microvascular involvement had a significantly higher blood flow. Volume perfusion CT has been shown to improve the detection of pancreatic insulinomas, particularly the ones which have transient hyperenhancement (comprising 30% cases)[60,61]. A recent study demonstrated that addition of low dose perfusion CT to contrast enhanced CT improved the detection rate of PNENs from 83.6% to 89.1% and found that blood flow parameters were significantly different between grade 1 and grade 2 tumors[62].

Perfusion CT has also been shown to have a role in monitoring response to treatment with antiangiogenic drugs. Few studies have shown that the perfusion parameters of PNENs and liver metastases decrease as early as 48 h after treatment with anti-angiogenic drugs and perfusion CT offers a significant role in an early noninvasive assessment[63,64]. A major limitation of perfusion CT is the higher radiation dose, resulting in an additional dose of approximately 7 mSv[65].

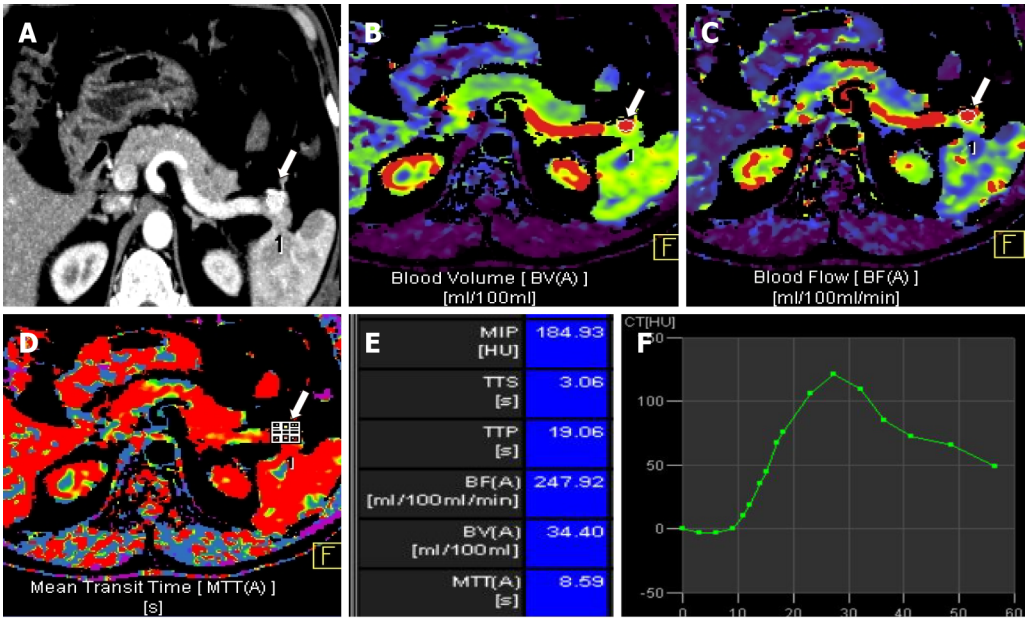

DOI: 10.3748/wjg.v28.i26.3008

Figure 4 Volume perfusion computed tomography images of a 56-year-old man with recurrent hyperinsulinemic hypoglycemia. A: Axial pancreatic phase computed tomography image shows a hyperenhancing lesion in the pancreatic tail (arrow); B-D: Color-coded parametric maps for blood volume (B), blood flow (C) and mean transit time (D) of the tumor (arrow) and normal pancreatic tissue; E: Chart shows mean value of each perfusion parameter of the tumor. Blood flow in the tumor was higher (247 mL/100 mL/min) compared to normal pancreatic parenchyma (72 mL/100 mL/min); F: Time attenuation curve shows dynamic enhancement pattern of the tumor corresponding to transient hyperenhancement. Histopathology after enucleation proved the tumor to be grade 1 insulinoma.

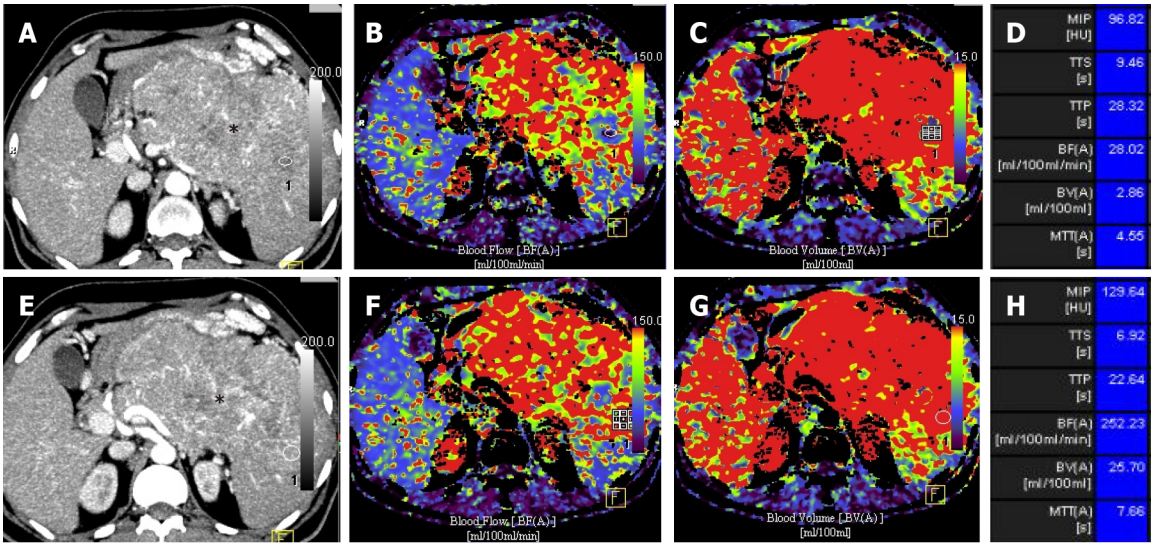

DOI: 10.3748/wjg.v28.i26.3008

Figure 5 Volume perfusion computed tomography images of a 67-year-old man with a large grade 3 neuroendocrine neoplasm involving body and tail of pancreas. A and B: Axial arterial phase computed tomography images with circular regions of interest placed at two different locations in the lesion (*); C-H: Parametric maps for blood flow (C and D) and blood volume (E and F) with mean value of each perfusion parameter (G and H) are shown. Lower values of mean blood flow, mean blood volume and mean transit time are features of high grade neuroendocrine neoplasm.

MRI

MRI is best performed as a problem-solving tool when CT scan findings are equivocal or negative, and is aimed at acquiring images of the lesion and organ with better soft tissue contrast. For instance, MRI has shown better sensitivity for the detection of liver metastases compared to CT and somatostatin receptor scintigraphy[66]. The absence of exposure to ionizing radiation makes MRI the apt modality for screening young individuals suspected of having NEN and those with syndromic association who require multiple follow up imaging[67]. Most NENs are hypointense on T1-weighted and hyperintense on T2-weighted images[10]. Contrast enhancement pattern and morphologic appearances are similar to

that seen in CT scan (Figure 6). For the detection of PNENs, the sensitivity of MRI ranges from 85% to 100% and specificity from 75% to 100%[68].

Diffusion-weighted imaging

Diffusion-weighted imaging (DWI) is a widely used technique in clinical imaging as it reflects the microscopic environment of the neoplasm including tumor cellularity and extracellular matrix. The application of DWI in oncology is mainly in tumor detection and assessing response to chemotherapy and radiotherapy. Wang *et al*[69] demonstrated that the apparent diffusion coefficient (ADC) values of PNEN correlated well with Ki-67 labelling index, thus indicating that DWI has a prognostic value (Figure 6). Another study showed that the ADC values were significantly different between benign and non-benign PNENs (1.48×10^{-3} mm^2/s *vs* 1.04×10^{-3} mm^2/s, respectively)[70]. Lotfalizadeh *et al*[71] showed that DWI has the additional value in identification of high grade tumors (grade 3) and can accurately differentiate grade 3 from grade 1/2 tumors (AUROC-0.96). The ADC values showed an inverse relation with the grade of the tumor.

Another major utility of DWI is in the detection and characterization of liver metastases. Several studies have shown that DWI is more sensitive for the detection of liver metastases than T2-weighted and multiphase gadolinium-enhanced MRI, especially for smaller lesions[72-74]. Besa *et al*[75] showed that the ADC of liver metastases from NEN weakly and significantly correlated negatively with tumor grade and Ki-67 and that the mean ADC and the minimum ADC values were significantly different between the three grades (1.6, 1.35 and 0.9×10^3 mm^2/s and 0.84, 0.5 and 0.27×10^3 mm^2/s for grades 1, 2 and 3, respectively). DWI is hence recommended in routine MRI abdomen protocol for the detection of liver metastases from NEN.

Histogram analysis of the ADC of the whole tumor has also been shown to predict tumor grade and aggressiveness. Pereira *et al*[76] found that whole tumor histogram analysis of the ADC, including the skewness and kurtosis can reliably differentiate grade 1 from grade 2/3 tumors. Another study also showed that this histogram analysis of ADC was useful in predicting tumor grade, vascular invasion and metastasis (node, liver) in PNENs and that $ADC_{entropy}$ and $ADC_{kurtosis}$ were the best markers in identifying tumor aggressiveness[77].

DWI is also useful in predicting and assessing response to various medical treatments for NENs. A recent study by Le Bihan *et al*[78] showed that the change in the ADC values of liver metastases from NENs after transarterial radioembolization was significantly different between the partial response and progressive disease groups, thus concluding that ADC can be used as an additional marker for treatment response evaluation.

While DWI investigates diffusion of water molecules in tissues, it does not detect perfusion of blood. Intravoxel incoherent motion (IVIM) DWI detects translational motion of water molecules in a voxel and can simultaneously quantify their diffusion and microcirculation in tissue capillary network[79]. IVIM images are quantified by ADC, which integrates the effects of both diffusion and perfusion. IVIM therefore enables evaluation of tissue perfusion without the requirement of a contrast agent. The quantitative parameters in IVIM include the pure diffusion coefficient (D_{slow}), which reflects the diffusion of water molecules, the pseudodiffusion coefficient (D_{fast}), which reflects the diffusion movement of capillary microcirculation perfusion, and the perfusion fraction (f), which represents the volume ratio between the perfusion effect of local microcirculation and the overall molecular diffusion (Figures 7 and 8). IVIM-DWI is a useful method to assess true tumor cellularity of PNEN, represented by tissue diffusion, as increased microcirculation of hypervascular PNENs may cause the pseudodiffusion effect and thus leads to the overestimation of ADC values[79]. Hwang *et al*[80] observed that IVIM DWI can differentiate grade 1 from grade 2 or 3 PNENs. They found that pure diffusion coefficient is a better marker of tumor cellularity than ADC, and was significantly higher in grade 1 PNENs, thereby enabling prediction of tumor grade on imaging. A recent study showed that D_{slow} and D_{fast} parameters help in the differentiation of high grade PNENs from pancreatic adenocarcinoma with high diagnostic accuracy (0.460 *vs* 0.579×10^3 mm^2/s and 13.361 *vs* 4.985×10^3 mm^2/s, respectively)[81].

Diffusion kurtosis imaging

Diffusion kurtosis imaging (DKI) is a new rapidly advancing MRI technique based on the concept that water molecules in biological environment have non Gaussian properties. This is in contrast to standard DWI that calculates ADC using monoexponential analysis, assuming that diffusion of water in tissues follows Gaussian behavior[82]. At higher b values (> 1000 s/mm^2), due to the barriers encountered by water molecules in tissues, there is deviation from Gaussian distribution. The deviation when quantified, in fact represents the tissue microenvironment. Two quantitative parameters, diffusion coefficient (D) and kurtosis (K), representing deviation from Gaussian distribution, can be extracted from DKI. DKI thus provides a more accurate model of diffusion and quantifies tissue heterogeneity, and irregularity of cellular microstructure by capturing non Gaussian diffusion parameters (Figure 9)[82,83]. A drawback which hampers its use in routine practice is the long acquisition time due to scan acquisition at multiple b values. There are studies showing application of DKI for the assessment of the pancreas[84,85]. Shi *et al*[83] found that the radiomics model of DKI and T2 weighted imaging could improve the diagnostic accuracy for PNENs.

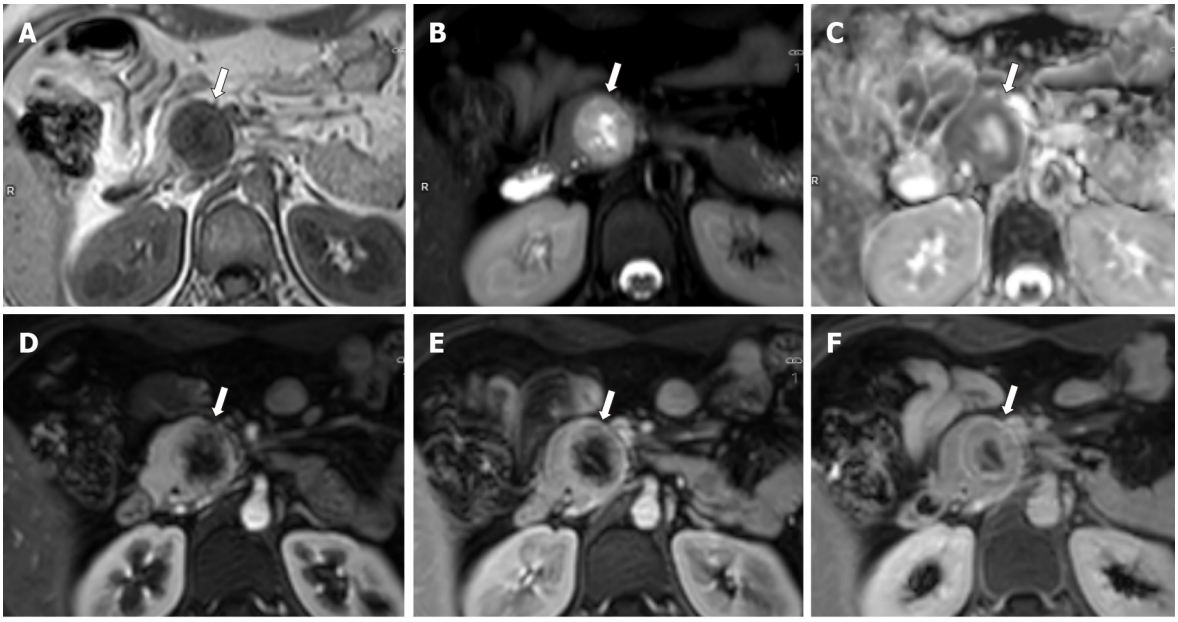

DOI: 10.3748/wjg.v28.i26.3008

Figure 6 Magnetic resonance images of a 24-year-old woman with multiple endocrine neoplasia-type 1 syndrome and pancreatic neuroendocrine neoplasm. A-C: Axial magnetic resonance images through the head of pancreas show a round heterogeneous mass (arrow) which appears hypointense on T1-weighted image (A), hyperintense on T2-weighted image with central cystic / necrotic change (B) and shows peripheral hypointensity on apparent diffusion coefficient (ADC) image (C) suggesting diffusion restriction along the periphery (ADC = 0.93 × 10^3 mm^2/s); D-F: Axial dynamic contrast enhanced T1-weighted images show hyperenhancement of the tumor along the periphery in pancreatic phase (D), with contrast retention in venous (E) and delayed (F) phase images. The patient also had bilateral inferior parathyroid and left superior parathyroid adenomas.

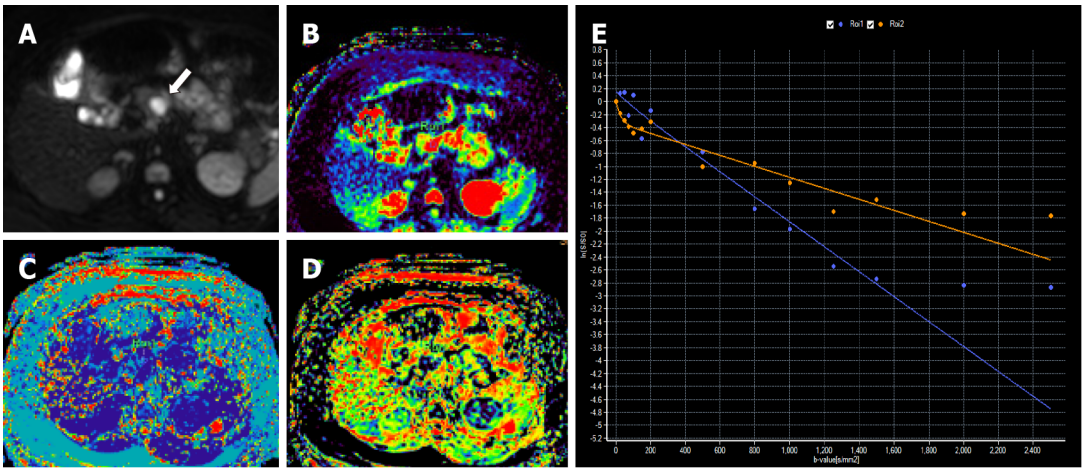

DOI: 10.3748/wjg.v28.i26.3008

Figure 7 Intravoxel incoherent motion diffusion-weighted imaging in a 46-year-old woman with proven grade 1 pancreatic neuroendocrine neoplasm. A: Axial diffusion weighted image (b = 800 s/mm^2) shows a small pancreatic lesion with diffusion restriction (arrow); B: Color-coded diffusion map shows true diffusion coefficient, D = 2.33 × 10^3 mm^2/s; C: Color-coded perfusion map shows pseudodiffusion coefficient, D* = 5.37 × 10^3 mm^2/s); D: Color-coded perfusion fraction map shows a value, f = 3.2%; E: Signal decay curve of the tumor (purple) shows fall in signal at lower b values with plateau at higher b values. In comparison, normal pancreas (orange) shows lesser diffusion restriction than the tumor.

MR elastography

MR elastography (MRE) is a phase-contrast-based MRI technique for the evaluation of mechanical tissue properties noninvasively, *e.g.,* tissue stiffness. MRE of pancreas is at an early stage. Recent studies have used MRE to differentiate healthy from pathological pancreatic tissue[86]. The normal pancreatic stiffness in adults measured by MRE is 1.1–1.21 kPa[86]. Shi *et al*[87] used MRE for the characterization of solid pancreatic masses. They found that malignant masses had significantly higher stiffness (3.27 kPa) than benign masses (1.96 kPa). PNENs had a median stiffness of 2.32 kPa. They also suggested that stiffness ratio (ratio of stiffness of mass to normal parenchyma) may perform better in the differentiation of benign from malignant pancreatic masses.

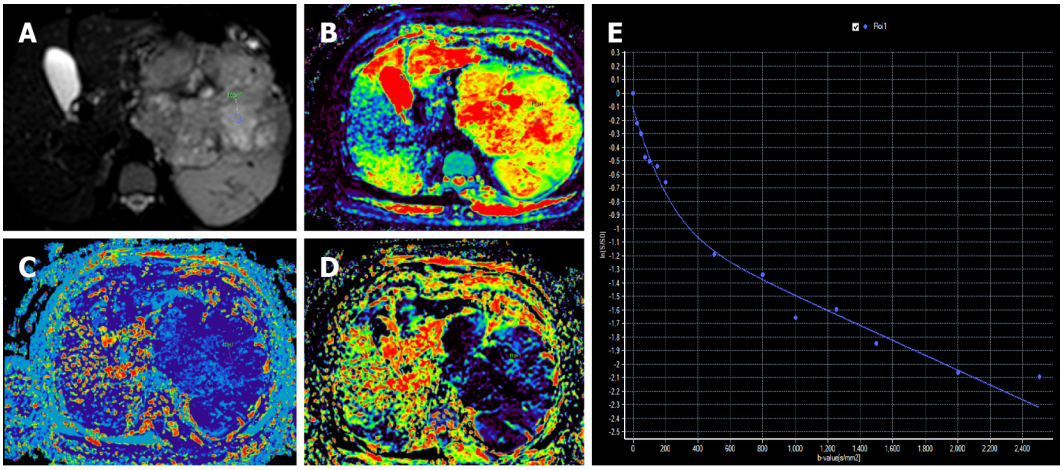

DOI: 10.3748/wjg.v28.i26.3008

Figure 8 Intravoxel incoherent motion diffusion-weighted imaging in a 67-year-old man with grade 3 pancreatic neuroendocrine neoplasm. A: Axial diffusion weighted image (b = 200 s/mm^2) with circular region of interest in the tumor; B: Color-coded diffusion map shows true diffusion coefficient, D = 0.84 × 10^3 mm^2/s; C: Color-coded perfusion map shows pseudodiffusion coefficient, D* = 5.01 × 10^3 mm^2/s); D: Color-coded perfusion fraction map shows a value, f = 4.5%; E: Signal decay curve shows steeper decay at low b values and continued fall at higher b values [in comparison to grade 1 pancreatic neuroendocrine neoplasm (PNEN) (Figure 7), true diffusion coefficient is lower in grade 3 PNENs].

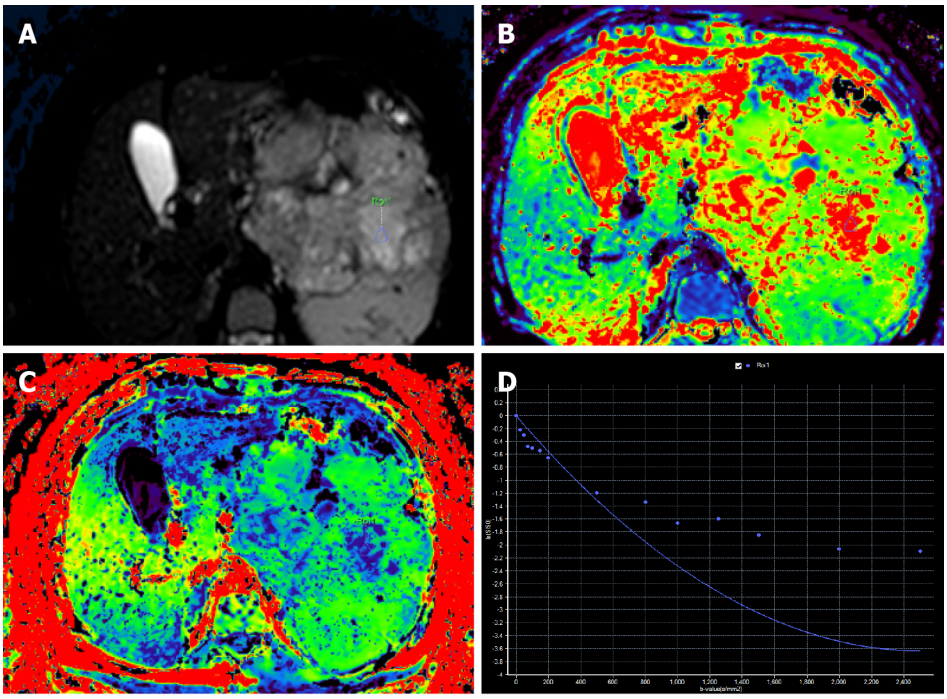

DOI: 10.3748/wjg.v28.i26.3008

Figure 9 Diffusion kurtosis of the lesion same as in Figure 8. A: Axial diffusion-weighted image (b = 200 s/mm^2) with region of interest marked; B: Diffusion map (D = 3 × 10^3 mm^2/s); C: Kurtosis map (k = 0.40); D: Signal decay curve shows non-Gaussian diffusion.

MRI perfusion

MRI perfusion techniques for the assessment of tumor perfusion have the major advantage that they lack adverse effects of radiation compared to the radiation-intensive CT perfusion. T1-weighted dynamic contrast enhanced (DCE) MRI is the technique applied in the evaluation of tumors in the abdomen[88]. This provides both semiquantitative and quantitative information on the microvascular perfusion of the tissue. The semiquantitative analysis is based on the time-signal intensity curve and the quantitative analysis is based on the Tofts two-compartment pharmacokinetic model (intravascular and extravascular-extracellular compartments) with the parameters evaluated being Ktrans (volume transfer constant, wash in), Kep (reverse efflux rate constant, wash out) and Ve (extravascular extracellular space volume fraction)[89]. This technique has shown promising results in the evaluation of PNENs. A study by Donati *et al*[90] showed that Ktrans and Kep values were higher in NENs (2.709 ± 0.110/min; 5.957 ±

0.371/min) compared to other focal lesions and healthy pancreatic parenchyma. This in fact reflects the wash in (Ktrans) and wash out (Kep) of the contrast agent from the hypervascular NENs. Also, well differentiated and poorly differentiated NENs showed different perfusion characteristics. In the study by Kim *et al*[91], Ktrans value of NENs were significantly higher than that of neuroendocrine carcinomas (0.339 ± 0.187/min *vs* 0.077 ± 0.036/min). Ductal adenocarcinomas being hypovascular, show significantly lower average values of Ktrans and Kep[90-92]. The role of DCE MRI in the evaluation of response to systemic chemotherapy and targeted molecular therapy by assessing the changes in the values of MRI perfusion parameters reflecting good or poor response to treatment is a direction for future studies.

PET CT AND PET MRI

Hybrid anatomical and functional imaging using PET/CT is a valuable tool in the current practice of grading and management of NENs. In general, in dual tracer PET/CT (somatostatin receptor imaging with Ga^{68} DOTATATE/TOC/NOC PET/CT and glucose metabolism with FDG PET/CT), low-grade tumors, which express somatostatin receptors, bind to somatostatin analog, but not to FDG[93]. In contrast, poorly differentiated GEPNENs with high Ki-67 index would be negative on somatostatin PET/CT but FDG avid[94]. Zhang *et al*[95] suggested that dual tracer PET /CT may be used as an alternative to tissue sampling, as it reflects both cellular somatostatin receptor expression and glucose metabolism. The authors also found a positive correlation between SUVmax (standardized uptake value) and Ki-67 index with respect to FDG PET/CT and negative correlation with respect to Ga^{68} DOTATATE PET/CT. However, low-grade insulinomas show low expression of somatostatin receptors in contrast to other secreting and nonsecreting NENs and are frequently not detected on Ga^{68} DOTATATE PET/CT[96]. Since virtually all benign insulinomas express glucagon-like peptide 1 (GLP-1) receptors (incretin receptors), these receptors can be targeted by PET/CT for preoperative localization of occult benign insulinomas. GLP-1R PET/CT had higher sensitivity than MRI and SPECT/CT for localization of benign insulinomas in a study by Antwi *et al*[97]. Glucose dependent insulinotropic polypeptide receptor (GIPR) is another incretin receptor overexpressed in GEPNENs. It is a potential target for imaging the small percentage (~10%) of GEPNENs which do not express SSTR and GLP1R, as confirmed by studies in animal models[98].

With technical advances, simultaneous PET and MRI acquisition in an integrated scanner is now possible. The first study in 2013 by Beiderwellen *et al*[99] showed that every lesion detected on PET/CT was identified on PET/MRI. Hope *et al*[100] evaluated hepatic lesions in patients with NENs using Ga^{68} DOTATOC PET/CT and PET/MRI and found that there was a strong correlation between SUVmax obtained in PET/CT and PET/MRI. However, due to the high cost, the routine use of PET/MRI is limited.

RADIOMICS, TEXTURE ANALYSIS AND MACHINE LEARNING

Radiomics is the process of conversion of digital biomedical images to mineable data and the subsequent analysis of this data[101]. Texture analysis is an imaging technique under the wider arena of radiomics, that extracts, analyzes and interprets quantitative imaging features, and enables objective assessment of tumor heterogeneity beyond what is possible to human eyes[102]. In statistical-based model of texture analysis, from each voxel in a region of interest, various first order (*e.g.*, first-order entropy, kurtosis, skewness, standard deviation, mean intensity) and second order (*e.g.*, contrast, uniformity, second order entropy, *etc.*), or higher order features are extracted and analyzed using post processing software. As mentioned previously, tumor grade is an important prognostic factor of NENs and their prediction noninvasively is valuable.

CT radiomics is increasingly finding its place in the grading of NENs. Canellas *et al*[103], evaluating PNENs on CT scan, found that tumors with high entropy (a texture parameter reflecting tissue heterogeneity) values had 3.7 times higher odds of being aggressive (grades 2 and 3). In this study, entropy was a better predictor of tumor grade than the size of the lesion. Choi *et al*[104] found that lower kurtosis, lower sphericity and higher skewness correlated to grade 2 or 3 PNENs. A study on 3D texture analysis of PNENs in 100 patients showed that kurtosis was significantly different between all the three grades and entropy could differentiate grade 1 from grade 3 and grade 2 from grade 3, but not grade 1 from grade 2 tumors[50]. These results of CT texture analysis were confirmed in other recent studies [105,106] thus emphasizing its role in the prediction of tumor grade.

MRI radiomics also help in characterizing PNENs. MRI texture analysis was found to be useful in differentiating nonfunctioning PNEN from solid pseudopapillary neoplasm in a study by Li *et al*[107]. Nonlinear discriminant analysis was found to have the lowest misclassification rate of all the types of analyses performed in their study. Shindo *et al*[108] studied ADC histogram for differentiation of pancreatic adenocarcinoma from PNENs. In their study, ADC entropy had the highest area under the curve (AUC) for differentiating adenocarcinoma from NEN. De Robertis *et al*[77] found that ADC

Table 3 Summary of important research studies on imaging of gastroenteropancreatic neuroendocrine neoplasms

	Ref.	Number (*n*)	Modality	Results	Conclusion
Ultrasonography	Takada *et al* [25], 2019	30	Contrast-enhanced harmonic EUS	Three parameters in TIC showed high diagnostic accuracy: Echo intensity change - 87%; Rate of enhancement - 87%; Enhancement ratio for node/pancreatic parenchyma - 88.5%	Contrast-enhanced EUS and TIC analysis show high diagnostic accuracy for grading of PNEN
CT	Worhunsky *et al*[45], 2014	118	APCT	5-year overall survival: Hypoenhancing - 54%; Isoenhancing - 89%; Hyperenhancin - 93%. On multivariate analysis only hypoenhancement (HR 2.32, P = 0.02) was independently associated with survival	Hypoenhancement of PNEN on APCT (22% of well-differentiated PNEN) was an independent predictor of poor outcome
	Rodallec *et al*[46], 2006	37	Dual-phase contrast-enhanced CT	Poorly differentiated NEC: Hypoattenuating - 71%; Isoattenuating or weakly hyperattenuating - 29%; Well-differentiated NECmoderately or strongly hyperattenuating - 53%. Poor enhancement at pancreatic phase and less vascularized tumors were associated with decreased survival rate	Enhancement of PNEN at CT correlated with microscopic tumor vascularity. Low-enhancing PNEN correlated with poor differentiation and lower overall survival
	Park *et al* [48], 2020	69	Dynamic CT	NEC (compared to well-differentiated NEN): Significantly higher frequencies of main pancreatic ductal dilatation, bile duct dilatation, vascular invasion; Significantly lower conspicuity of interface between tumor and parenchyma, AER and PER. PER < 0.8 showed 94.1% sensitivity, 88.5% specificity for differentiation of NEC from well-differentiated NEN. On combining 3 significant CT features, the sensitivity and specificity for diagnosing NEC were 88.2% and 88.5% respectively	Tumor parenchyma enhancement ratio in portal phase is useful to distinguish NECs from well differentiated NENs. Combining qualitative and quantitative CT features aid in achieving good diagnostic accuracy in differentiation between NEC and well-differentiated NEN
	d'Assignies *et al*[59], 2009	36	MDCT perfusion	Tumor blood flow and intratumoral MVD showed high correlation (r = 0.620, P < 0.001). Blood flow was significantly higher in: Grade 1 than grade 2/3 tumors; Tumors with proliferation index ≤ 2% (P = 0.005); Tumors without histological signs of microscopic vascular involvement (P = 0.008). Mean transit time was longer in tumors with lymph node (P = 0.02) or liver (P = 0.05) metastasis	Perfusion CT is feasible in patients with pancreatic NENs and reflects MVD. Perfusion CT measurements correlated with histoprognostic factors, such as proliferation index and WHO grading
MRI	Canellas *et al*[103], 2018	80	MRI	MRI features associated with aggressive tumors: Size > 2 cm (OR = 4.8); T2 non-bright lesions (OR = 4.6); Presence of pancreatic ductal dilatation (OR = 4.9); Diffusion restriction (OR = 4.9)	MRI can assess aggressiveness of PNEN and identify patients at risk for early disease progression after surgical resection
	d'Assignies *et al*[74], 2013	59	MRI	DWI (71%-71.6%) was more sensitive than T2 weighted images (55.6%) and dynamic CEMRI (47.5%-48.1%). Combination of these sequences improved detection of liver metastases. Specificity of each sequence was comparable (89%-100%)	DWI is more sensitive for detection and characterization of liver metastases from NENs than T2-weighted and dynamic gadolinium-enhanced MRI
Radiomics, texture analysis and machine learning	Canellas *et al*[103], 2018	101	CECT with texture analysis	CT features predictive of a more aggressive tumor: Size > 2 cm (OR = 3.3); Vascular involvement (OR = 25.2); Pancreatic ductal dilatation (OR = 6); Lymphadenopathy (OR = 6.8); Entropy (OR = 3.7); Differences (P < 0.05) in progression free survival were found for: Grade 1 *vs* grade 2 *vs* grade 3 tumors; PNEN with vascular involvement; Tumors with entropy values > 4.65	CT texture analysis and CT features are predictive of aggressiveness and can be used to identify patients at risk of early disease progression after surgical resection
	De Robertis *et al*[77], 2018	42	MRI and histogram analysis	ADC entropy is significantly higher in grade 2/3 tumors (sensitivity: 83.3%, specificity: 61.1%). ADC kurtosis is higher in PNENs with vascular involvement, nodal and hepatic metastases (sensitivity: 85.7%, specificity: 74.3%)	Whole tumor ADC histogram analysis can predict aggressiveness in PNENs. ADC entropy and ADC kurtosis are the most accurate parameters for identification of PNEN with malignant behavior
	Luo *et al* [112], 2020	93	CECT with application of a CNN based DL algorithm	AUC = 0.81 of arterial phase in validation set was significantly higher than those of venous (AUC = 0.57, P = 0.03) and arterial/venous phase (AUC = 0.70, P = 0.03) in predicting the pathological grading of PNENs. The AUC and accuracy of DL algorithm for diagnosing grade 3 PNEN were 0.80% and 79.1%. There was significant difference in OS and PFS between the predicted G1/2 and G3 groups	The CNN-based DL method showed a relatively robust performance in predicting pathological grading of PNENs from CECT images
	Gao *et al*	96	CEMRI with	The average accuracy of the five trained CNNs	With the help of GAN, the CNN

	[114], 2019	application of deep learning algorithm on images	ranged between 79.08% and 82.35%, and the range of micro- average AUC was between 0.8825 and 0.8932. The average accuracy and micro-average AUC of the averaged CNN were 81.05% and 0.8847 respectively	showed the potential to predict the grades of PNENs on CEMRI

EUS: Enhanced ultrasonography; TIC: Time-signal intensity curve; APCT: Arterial phase computed tomography; ADC: Apparent diffusion coefficient; CECT: Contrast enhanced computed tomography; CEMRI: Contrast enhanced magnetic resonance imaging; CNN: Convolutional neural network; DWI: Diffusion weighted imaging; NEC: Neuroendocrine carcinoma; NEN: Neuroendocrine neoplasm; AER: Annual equivalent ratio; PER: Portal enhancement ratio; MVD: Microvascular density; WHO: World Health Organization; MDCT: Multidetector row computed tomography; OS: Overall survival; PFS: Progression free survival; AUC: Area under the curve; PNEN: Pancreatic neuroendocrine neoplasm; GAN: Generative Adversarial Network.

histogram analysis of DWI, using radiomics, could predict aggressiveness of PNENs. They found high ADC kurtosis values in tumors with vascular invasion (AUC of 0.763 for a cut off value of 4.13) and distant metastases (AUC of 0.820 for a cut off of 3.642)[77]. The future prospects of radiomics are in the direction of development of a robust predictive model combining qualitative and quantitative imaging parameters.

Machine learning is increasingly being used in medicine and has various applications including detection of disease, classification of images, identifying treatment and monitoring adherence to therapy [109,110]. The standard radiomics analysis on CT or MRI requires marking of the tumor margins for analysis. However, deep learning using convolutional neural network (CNN) performs analysis automatically and provides better results[111]. A few recent preliminary studies have shown the promising role of deep learning using CNN in the prediction of grade of PNEN and survival using contrast enhanced CT[112-114]. Clinical trials for translation of these imaging techniques into clinical practice and validation for routine use are ongoing.

In short, the quantitative parameters derived from imaging, relevant for prognostication of GEPNENs include tumor size, enhancement ratios derived from HU values, iodine uptake on DECT, entropy on CT texture analysis, tumor blood flow, tumor blood volume, and mean transit time on perfusion CT, ADC and ADC histogram analysis of DWI, true and pseudodiffusion coefficients and perfusion fraction on IVIM DWI, Ktrans and Kep on perfusion MRI and SUVmax on dual tracer PET/CT. A combination of qualitative features and quantitative factors with the newer functional imaging techniques enables better tumor classification based on their prognosis. A summary of important studies on advanced imaging in GEPNENs is shown in Table 3.

CONCLUSION

With the recent advances in CT, MRI, USG and hybrid imaging techniques like PET/CT and PET/MRI using dual tracers, smaller pancreatic and bowel NENs are now being increasingly detected and staged. In addition to tumor detection and staging, their non-invasive grading, prognostication and monitoring response to treatment are shown to be feasible and reliable with the emerging studies using quantitative imaging techniques like CT and MR perfusion studies, DWI, IVIM and texture analysis with radiomics. Standardization of these techniques with more large scale studies would be an important future prospect. These advances in imaging will help in making the right treatment choice, contributing to an overall improvement in patient outcome.

FOOTNOTES

Author contributions: Ramachandran A contributed to initial draft and revision; Madhusudhan KS contributed to review of draft and revision.

Conflict-of-interest statement: No conflict of interests.

Country/Territory of origin: India

ORCID number: Anupama Ramachandran 0000-0002-5808-6076; Kumble Seetharama Madhusudhan 0000-0001-8806-2625.

Corresponding Author's Membership in Professional Societies: Indian Radiological and Imaging Association, No.

501LM/D-285A.

S-Editor: Zhang H
L-Editor: Kerr C
P-Editor: Zhang H

REFERENCES

1 **Lawrence B**, Gustafsson BI, Chan A, Svejda B, Kidd M, Modlin IM. The epidemiology of gastroenteropancreatic neuroendocrine tumors. *Endocrinol Metab Clin North Am* 2011; **40**: 1-18, vii [PMID: 21349409 DOI: 10.1016/j.ecl.2010.12.005]
2 **Turaga KK**, Kvols LK. Recent progress in the understanding, diagnosis, and treatment of gastroenteropancreatic neuroendocrine tumors. *CA Cancer J Clin* 2011; **61**: 113-132 [PMID: 21388967 DOI: 10.3322/caac.20097]
3 **Modlin IM**, Lye KD, Kidd M. A 5-decade analysis of 13,715 carcinoid tumors. *Cancer* 2003; **97**: 934-959 [PMID: 12569593 DOI: 10.1002/cncr.11105]
4 **Sahani DV**, Bonaffini PA, Fernández-Del Castillo C, Blake MA. Gastroenteropancreatic neuroendocrine tumors: role of imaging in diagnosis and management. *Radiology* 2013; **266**: 38-61 [PMID: 23264526 DOI: 10.1148/radiol.12112512]
5 **Toumpanakis CG**, Caplin ME. Molecular genetics of gastroenteropancreatic neuroendocrine tumors. *Am J Gastroenterol* 2008; **103**: 729-732 [PMID: 18341492 DOI: 10.1111/j.1572-0241.2007.01777.x]
6 **Gallotti A**, Johnston RP, Bonaffini PA, Ingkakul T, Deshpande V, Fernández-del Castillo C, Sahani DV. Incidental neuroendocrine tumors of the pancreas: MDCT findings and features of malignancy. *AJR Am J Roentgenol* 2013; **200**: 355-362 [PMID: 23345357 DOI: 10.2214/AJR.11.8037]
7 **Nagtegaal ID**, Odze RD, Klimstra D, Paradis V, Rugge M, Schirmacher P, Washington KM, Carneiro F, Cree IA; WHO Classification of Tumours Editorial Board. The 2019 WHO classification of tumours of the digestive system. *Histopathology* 2020; **76**: 182-188 [PMID: 31433515 DOI: 10.1111/his.13975]
8 **Kunz PL**, Reidy-Lagunes D, Anthony LB, Bertino EM, Brendtro K, Chan JA, Chen H, Jensen RT, Kim MK, Klimstra DS, Kulke MH, Liu EH, Metz DC, Phan AT, Sippel RS, Strosberg JR, Yao JC; North American Neuroendocrine Tumor Society. Consensus guidelines for the management and treatment of neuroendocrine tumors. *Pancreas* 2013; **42**: 557-577 [PMID: 23591432 DOI: 10.1097/MPA.0b013e31828e34a4]
9 **Falconi M**, Eriksson B, Kaltsas G, Bartsch DK, Capdevila J, Caplin M, Kos-Kudla B, Kwekkeboom D, Rindi G, Klöppel G, Reed N, Kianmanesh R, Jensen RT; Vienna Consensus Conference participants. ENETS Consensus Guidelines Update for the Management of Patients with Functional Pancreatic Neuroendocrine Tumors and Non-Functional Pancreatic Neuroendocrine Tumors. *Neuroendocrinology* 2016; **103**: 153-171 [PMID: 26742109 DOI: 10.1159/000443171]
10 **Tan EH**, Tan CH. Imaging of gastroenteropancreatic neuroendocrine tumors. *World J Clin Oncol* 2011; **2**: 28-43 [PMID: 21603312 DOI: 10.5306/wjco.v2.i1.28]
11 **Modlin IM**, Oberg K, Chung DC, Jensen RT, de Herder WW, Thakker RV, Caplin M, Delle Fave G, Kaltsas GA, Krenning EP, Moss SF, Nilsson O, Rindi G, Salazar R, Ruszniewski P, Sundin A. Gastroenteropancreatic neuroendocrine tumours. *Lancet Oncol* 2008; **9**: 61-72 [PMID: 18177818 DOI: 10.1016/S1470-2045(07)70410-2]
12 **Giovannini M**. Contrast-enhanced and 3-dimensional endoscopic ultrasonography. *Gastroenterol Clin North Am* 2010; **39**: 845-858 [PMID: 21093759 DOI: 10.1016/j.gtc.2010.08.027]
13 **Takeda K**, Goto H, Hirooka Y, Itoh A, Hashimoto S, Niwa K, Hayakawa T. Contrast-enhanced transabdominal ultrasonography in the diagnosis of pancreatic mass lesions. *Acta Radiol* 2003; **44**: 103-106 [PMID: 12631008]
14 **Malagò R**, D'Onofrio M, Zamboni GA, Faccioli N, Falconi M, Boninsegna L, Mucelli RP. Contrast-enhanced sonography of nonfunctioning pancreatic neuroendocrine tumors. *AJR Am J Roentgenol* 2009; **192**: 424-430 [PMID: 19155405 DOI: 10.2214/AJR.07.4043]
15 **Del Prete M**, Di Sarno A, Modica R, Lassandro F, Giorgio A, Bianco A, Muto M, Gasperi M, Del Prete F, Colao A, Montesarchio V, Faggiano A; ENETS Centre of Excellence Multidisciplinary Group for Neuroendocrine Tumors in Naples (Italy). Role of contrast-enhanced ultrasound to define prognosis and predict response to biotherapy in pancreatic neuroendocrine tumors. *J Endocrinol Invest* 2017; **40**: 1373-1380 [PMID: 28667452 DOI: 10.1007/s40618-017-0723-x]
16 **Giovannini M**, Hookey LC, Bories E, Pesenti C, Monges G, Delpero JR. Endoscopic ultrasound elastography: the first step towards virtual biopsy? *Endoscopy* 2006; **38**: 344-348 [PMID: 16680632 DOI: 10.1055/s-2006-925158]
17 **Park MK**, Jo J, Kwon H, Cho JH, Oh JY, Noh MH, Nam KJ. Usefulness of acoustic radiation force impulse elastography in the differential diagnosis of benign and malignant solid pancreatic lesions. *Ultrasonography* 2014; **33**: 26-33 [PMID: 24936492 DOI: 10.14366/usg.13017]
18 **Uchida H**, Hirooka Y, Itoh A, Kawashima H, Hara K, Nonogaki K, Kasugai T, Ohno E, Ohmiya N, Niwa Y, Katano Y, Ishigami M, Goto H. Feasibility of tissue elastography using transcutaneous ultrasonography for the diagnosis of pancreatic diseases. *Pancreas* 2009; **38**: 17-22 [PMID: 18695627 DOI: 10.1097/MPA.0b013e318184db78]
19 **Hunt GC**, Faigel DO. Assessment of EUS for diagnosing, staging, and determining resectability of pancreatic cancer: a review. *Gastrointest Endosc* 2002; **55**: 232-237 [PMID: 11818928 DOI: 10.1067/mge.2002.121342]
20 **Legmann P**, Vignaux O, Dousset B, Baraza AJ, Palazzo L, Dumontier I, Coste J, Louvel A, Roseau G, Couturier D, Bonnin A. Pancreatic tumors: comparison of dual-phase helical CT and endoscopic sonography. *AJR Am J Roentgenol* 1998; **170**: 1315-1322 [PMID: 9574609 DOI: 10.2214/ajr.170.5.9574609]
21 **Rösch T**, Lightdale CJ, Botet JF, Boyce GA, Sivak MV Jr, Yasuda K, Heyder N, Palazzo L, Dancygier H, Schusdziarra V. Localization of pancreatic endocrine tumors by endoscopic ultrasonography. *N Engl J Med* 1992; **326**: 1721-1726 [PMID: 1317506 DOI: 10.1056/NEJM199206253262601]
22 **Kim MK**. Endoscopic ultrasound in gastroenteropancreatic neuroendocrine tumors. *Gut Liver* 2012; **6**: 405-410 [PMID:

23170141 DOI: 10.5009/gnl.2012.6.4.405]
23 **Anderson MA**, Carpenter S, Thompson NW, Nostrant TT, Elta GH, Scheiman JM. Endoscopic ultrasound is highly accurate and directs management in patients with neuroendocrine tumors of the pancreas. *Am J Gastroenterol* 2000; **95**: 2271-2277 [PMID: 11007228 DOI: 10.1111/j.1572-0241.2000.02480.x]
24 **Guo J**, Sahai AV, Teoh A, Arcidiacono PG, Larghi A, Saftoiu A, Siddiqui AA, Arturo Arias BL, Jenssen C, Adler DG, Lakhtakia S, Seo DW, Itokawa F, Giovannini M, Mishra G, Sabbagh L, Irisawa A, Iglesias-Garcia J, Poley JW, Vila JJ, Jesse L, Kubota K, Kalaitzakis E, Kida M, El-Nady M, Mukai SU, Ogura T, Fusaroli P, Vilmann P, Rai P, Nguyen NQ, Ponnudurai R, Achanta CR, Baron TH, Yasuda I, Wang HP, Hu J, Duan B, Bhutani MS, Sun S. An international, multi-institution survey on performing EUS-FNA and fine needle biopsy. *Endosc Ultrasound* 2020; **9**: 319-328 [PMID: 32883921 DOI: 10.4103/eus.eus_56_20]
25 **Takada S**, Kato H, Saragai Y, Muro S, Uchida D, Tomoda T, Matsumoto K, Horiguchi S, Tanaka N, Okada H. Contrast-enhanced harmonic endoscopic ultrasound using time-intensity curve analysis predicts pathological grade of pancreatic neuroendocrine neoplasm. *J Med Ultrason (2001)* 2019; **46**: 449-458 [PMID: 31377939 DOI: 10.1007/s10396-019-00967-x]
26 **Janssen J**, Schlörer E, Greiner L. EUS elastography of the pancreas: feasibility and pattern description of the normal pancreas, chronic pancreatitis, and focal pancreatic lesions. *Gastrointest Endosc* 2007; **65**: 971-978 [PMID: 17531630 DOI: 10.1016/j.gie.2006.12.057]
27 **Săftoiu A**, Vilmann P, Gorunescu F, Gheonea DI, Gorunescu M, Ciurea T, Popescu GL, Iordache A, Hassan H, Iordache S. Neural network analysis of dynamic sequences of EUS elastography used for the differential diagnosis of chronic pancreatitis and pancreatic cancer. *Gastrointest Endosc* 2008; **68**: 1086-1094 [PMID: 18656186 DOI: 10.1016/j.gie.2008.04.031]
28 **Hirche TO**, Ignee A, Barreiros AP, Schreiber-Dietrich D, Jungblut S, Ott M, Hirche H, Dietrich CF. Indications and limitations of endoscopic ultrasound elastography for evaluation of focal pancreatic lesions. *Endoscopy* 2008; **40**: 910-917 [PMID: 19009483 DOI: 10.1055/s-2008-1077726]
29 **Havre RF**, Ødegaard S, Gilja OH, Nesje LB. Characterization of solid focal pancreatic lesions using endoscopic ultrasonography with real-time elastography. *Scand J Gastroenterol* 2014; **49**: 742-751 [PMID: 24713038 DOI: 10.3109/00365521.2014.905627]
30 **Micames CG**, Gress FG. EUS elastography: a step ahead? *Gastrointest Endosc* 2007; **65**: 979-981 [PMID: 17531631 DOI: 10.1016/j.gie.2007.02.059]
31 **Ohno E**, Hirooka Y, Kawashima H, Ishikawa T. Feasibility of EUS-guided shear-wave measurement: A preliminary clinical study. *Endosc Ultrasound* 2019; **8**: 215-216 [PMID: 30924448 DOI: 10.4103/eus.eus_6_19]
32 **Yamashita Y**, Tanioka K, Kawaji Y, Tamura T, Nuta J, Hatamaru K, Itonaga M, Yoshida T, Ida Y, Maekita T, Iguchi M, Kitano M. Utility of Elastography with Endoscopic Ultrasonography Shear-Wave Measurement for Diagnosing Chronic Pancreatitis. *Gut Liver* 2020; **14**: 659-664 [PMID: 31722469 DOI: 10.5009/gnl19170]
33 **Ohno E**, Kawashima H, Ishikawa T, Iida T, Suzuki H, Uetsuki K, Yashika J, Yamada K, Yoshikawa M, Gibo N, Aoki T, Kataoka K, Mori H, Yamamura T, Furukawa K, Nakamura M, Hirooka Y, Fujishiro M. Diagnostic performance of endoscopic ultrasonography-guided elastography for solid pancreatic lesions: Shear-wave measurements versus strain elastography with histogram analysis. *Dig Endosc* 2021; **33**: 629-638 [PMID: 32662150 DOI: 10.1111/den.13791]
34 **Manguso N**, Gangi A, Johnson J, Harit A, Nissen N, Jamil L, Lo S, Wachsman A, Hendifar A, Amersi F. The role of pre-operative imaging and double balloon enteroscopy in the surgical management of small bowel neuroendocrine tumors: Is it necessary? *J Surg Oncol* 2018; **117**: 207-212 [PMID: 28940412 DOI: 10.1002/jso.24825]
35 **Malla S**, Kumar P, Madhusudhan KS. Radiology of the neuroendocrine neoplasms of the gastrointestinal tract: a comprehensive review. *Abdom Radiol (NY)* 2021; **46**: 919-935 [PMID: 32960304 DOI: 10.1007/s00261-020-02773-3]
36 **Bonekamp D**, Raman SP, Horton KM, Fishman EK. Role of computed tomography angiography in detection and staging of small bowel carcinoid tumors. *World J Radiol* 2015; **7**: 220-235 [PMID: 26435774 DOI: 10.4329/wjr.v7.i9.220]
37 **Kamaoui I**, De-Luca V, Ficarelli S, Mennesson N, Lombard-Bohas C, Pilleul F. Value of CT enteroclysis in suspected small-bowel carcinoid tumors. *AJR Am J Roentgenol* 2010; **194**: 629-633 [PMID: 20173138 DOI: 10.2214/AJR.09.2760]
38 **Hakim FA**, Alexander JA, Huprich JE, Grover M, Enders FT. CT-enterography may identify small bowel tumors not detected by capsule endoscopy: eight years experience at Mayo Clinic Rochester. *Dig Dis Sci* 2011; **56**: 2914-2919 [PMID: 21735085 DOI: 10.1007/s10620-011-1773-0]
39 **Huprich JE**, Fletcher JG, Fidler JL, Alexander JA, Guimarães LS, Siddiki HA, McCollough CH. Prospective blinded comparison of wireless capsule endoscopy and multiphase CT enterography in obscure gastrointestinal bleeding. *Radiology* 2011; **260**: 744-751 [PMID: 21642417 DOI: 10.1148/radiol.11110143]
40 **Dromain C**, de Baere T, Baudin E, Galline J, Ducreux M, Boige V, Duvillard P, Laplanche A, Caillet H, Lasser P, Schlumberger M, Sigal R. MR imaging of hepatic metastases caused by neuroendocrine tumors: comparing four techniques. *AJR Am J Roentgenol* 2003; **180**: 121-128 [PMID: 12490490 DOI: 10.2214/ajr.180.1.1800121]
41 **Paulson EK**, McDermott VG, Keogan MT, DeLong DM, Frederick MG, Nelson RC. Carcinoid metastases to the liver: role of triple-phase helical CT. *Radiology* 1998; **206**: 143-150 [PMID: 9423664 DOI: 10.1148/radiology.206.1.9423664]
42 **Horton KM**, Kamel I, Hofmann L, Fishman EK. Carcinoid tumors of the small bowel: a multitechnique imaging approach. *AJR Am J Roentgenol* 2004; **182**: 559-567 [PMID: 14975946 DOI: 10.2214/ajr.182.3.1820559]
43 **Manfredi R**, Bonatti M, Mantovani W, Graziani R, Segala D, Capelli P, Butturini G, Mucelli RP. Non-hyperfunctioning neuroendocrine tumours of the pancreas: MR imaging appearance and correlation with their biological behaviour. *Eur Radiol* 2013; **23**: 3029-3039 [PMID: 23793519 DOI: 10.1007/s00330-013-2929-4]
44 **Humphrey PE**, Alessandrino F, Bellizzi AM, Mortele KJ. Non-hyperfunctioning pancreatic endocrine tumors: multimodality imaging features with histopathological correlation. *Abdom Imaging* 2015; **40**: 2398-2410 [PMID: 25989932 DOI: 10.1007/s00261-015-0458-0]
45 **Worhunsky DJ**, Krampitz GW, Poullos PD, Visser BC, Kunz PL, Fisher GA, Norton JA, Poultsides GA. Pancreatic neuroendocrine tumours: hypoenhancement on arterial phase computed tomography predicts biological aggressiveness. *HPB (Oxford)* 2014; **16**: 304-311 [PMID: 23991643 DOI: 10.1111/hpb.12139]

46 **Rodallec M**, Vilgrain V, Couvelard A, Rufat P, O'Toole D, Barrau V, Sauvanet A, Ruszniewski P, Menu Y. Endocrine pancreatic tumours and helical CT: contrast enhancement is correlated with microvascular density, histoprognostic factors and survival. *Pancreatology* 2006; **6**: 77-85 [PMID: 16327283 DOI: 10.1159/000090026]

47 **Kim DW**, Kim HJ, Kim KW, Byun JH, Song KB, Kim JH, Hong SM. Neuroendocrine neoplasms of the pancreas at dynamic enhanced CT: comparison between grade 3 neuroendocrine carcinoma and grade 1/2 neuroendocrine tumour. *Eur Radiol* 2015; **25**: 1375-1383 [PMID: 25465713 DOI: 10.1007/s00330-014-3532-z]

48 **Park HJ**, Kim HJ, Kim KW, Kim SY, Choi SH, You MW, Hwang HS, Hong SM. Comparison between neuroendocrine carcinomas and well-differentiated neuroendocrine tumors of the pancreas using dynamic enhanced CT. *Eur Radiol* 2020; **30**: 4772-4782 [PMID: 32346794 DOI: 10.1007/s00330-020-06867-w]

49 **Yamada S**, Fujii T, Suzuki K, Inokawa Y, Kanda M, Nakayama G, Sugimoto H, Koike M, Nomoto S, Fujiwara M, Nakao A, Kodera Y. Preoperative Identification of a Prognostic Factor for Pancreatic Neuroendocrine Tumors Using Multiphase Contrast-Enhanced Computed Tomography. *Pancreas* 2016; **45**: 198-203 [PMID: 26390421 DOI: 10.1097/MPA.0000000000000443]

50 **D'Onofrio M**, Ciaravino V, Cardobi N, De Robertis R, Cingarlini S, Landoni L, Capelli P, Bassi C, Scarpa A. CT Enhancement and 3D Texture Analysis of Pancreatic Neuroendocrine Neoplasms. *Sci Rep* 2019; **9**: 2176 [PMID: 30778137 DOI: 10.1038/s41598-018-38459-6]

51 **Hardie AD**, Picard MM, Camp ER, Perry JD, Suranyi P, De Cecco CN, Schoepf UJ, Wichmann JL. Application of an Advanced Image-Based Virtual Monoenergetic Reconstruction of Dual Source Dual-Energy CT Data at Low keV Increases Image Quality for Routine Pancreas Imaging. *J Comput Assist Tomogr* 2015; **39**: 716-720 [PMID: 26196343 DOI: 10.1097/RCT.0000000000000276]

52 **Lin XZ**, Wu ZY, Tao R, Guo Y, Li JY, Zhang J, Chen KM. Dual energy spectral CT imaging of insulinoma-Value in preoperative diagnosis compared with conventional multi-detector CT. *Eur J Radiol* 2012; **81**: 2487-2494 [PMID: 22153746 DOI: 10.1016/j.ejrad.2011.10.028]

53 **Kaltenbach B**, Wichmann JL, Pfeifer S, Albrecht MH, Booz C, Lenga L, Hammerstingl R, D'Angelo T, Vogl TJ, Martin SS. Iodine quantification to distinguish hepatic neuroendocrine tumor metastasis from hepatocellular carcinoma at dual-source dual-energy liver CT. *Eur J Radiol* 2018; **105**: 20-24 [PMID: 30017280 DOI: 10.1016/j.ejrad.2018.05.019]

54 **Kambadakone AR**, Sahani DV. Body perfusion CT: technique, clinical applications, and advances. *Radiol Clin North Am* 2009; **47**: 161-178 [PMID: 19195541 DOI: 10.1016/j.rcl.2008.11.003]

55 **Sinitsyn V**. Analysis and Interpretation of Perfusion CT in Oncology: Type of Cancer Matters. *Radiology* 2019; **292**: 636-637 [PMID: 31287775 DOI: 10.1148/radiol.2019191265]

56 **Marion-Audibert AM**, Barel C, Gouysse G, Dumortier J, Pilleul F, Pourreyron C, Hervieu V, Poncet G, Lombard-Bohas C, Chayvialle JA, Partensky C, Scoazec JY. Low microvessel density is an unfavorable histoprognostic factor in pancreatic endocrine tumors. *Gastroenterology* 2003; **125**: 1094-1104 [PMID: 14517793 DOI: 10.1016/s0016-5085(03)01198-3]

57 **Couvelard A**, O'Toole D, Turley H, Leek R, Sauvanet A, Degott C, Ruszniewski P, Belghiti J, Harris AL, Gatter K, Pezzella F. Microvascular density and hypoxia-inducible factor pathway in pancreatic endocrine tumours: negative correlation of microvascular density and VEGF expression with tumour progression. *Br J Cancer* 2005; **92**: 94-101 [PMID: 15558070 DOI: 10.1038/sj.bjc.6602245]

58 **Takahashi Y**, Akishima-Fukasawa Y, Kobayashi N, Sano T, Kosuge T, Nimura Y, Kanai Y, Hiraoka N. Prognostic value of tumor architecture, tumor-associated vascular characteristics, and expression of angiogenic molecules in pancreatic endocrine tumors. *Clin Cancer Res* 2007; **13**: 187-196 [PMID: 17200354 DOI: 10.1158/1078-0432.CCR-06-1408]

59 **d'Assignies G**, Couvelard A, Bahrami S, Vullierme MP, Hammel P, Hentic O, Sauvanet A, Bedossa P, Ruszniewski P, Vilgrain V. Pancreatic endocrine tumors: tumor blood flow assessed with perfusion CT reflects angiogenesis and correlates with prognostic factors. *Radiology* 2009; **250**: 407-416 [PMID: 19095784 DOI: 10.1148/radiol.2501080291]

60 **Zhu L**, Wu WM, Xue HD, Liu W, Wang X, Sun H, Li P, Zhao YP, Jin ZY. Sporadic insulinomas on volume perfusion CT: dynamic enhancement patterns and timing of optimal tumour-parenchyma contrast. *Eur Radiol* 2017; **27**: 3491-3498 [PMID: 28108839 DOI: 10.1007/s00330-016-4709-4]

61 **Zhu L**, Xue H, Sun H, Wang X, Wu W, Jin Z, Zhao Y. Insulinoma Detection With MDCT: Is There a Role for Whole-Pancreas Perfusion? *AJR Am J Roentgenol* 2017; **208**: 306-314 [PMID: 27929662 DOI: 10.2214/AJR.16.16351]

62 **Wan Y**, Hao H, Meng S, Li Z, Yu F, Meng Chi, Chao Q, Gao J. Application of low dose pancreas perfusion CT combined with enhancement scanning in diagnosis of pancreatic neuroendocrine tumors. *Pancreatology* 2021; **21**: 240-245 [PMID: 33191144 DOI: 10.1016/j.pan.2020.10.046]

63 **Ng CS**, Charnsangavej C, Wei W, Yao JC. Perfusion CT findings in patients with metastatic carcinoid tumors undergoing bevacizumab and interferon therapy. *AJR Am J Roentgenol* 2011; **196**: 569-576 [PMID: 21343498 DOI: 10.2214/AJR.10.4455]

64 **Ng CS**, Wei W, Duran C, Ghosh P, Anderson EF, Chandler AG, Yao JC. CT perfusion in normal liver and liver metastases from neuroendocrine tumors treated with targeted antivascular agents. *Abdom Radiol (NY)* 2018; **43**: 1661-1669 [PMID: 29075824 DOI: 10.1007/s00261-017-1367-1]

65 **Ketelsen D**, Horger M, Buchgeister M, Fenchel M, Thomas C, Boehringer N, Schulze M, Tsiflikas I, Claussen CD, Heuschmid M. Estimation of radiation exposure of 128-slice 4D-perfusion CT for the assessment of tumor vascularity. *Korean J Radiol* 2010; **11**: 547-552 [PMID: 20808699 DOI: 10.3348/kjr.2010.11.5.547]

66 **Dromain C**, de Baere T, Lumbroso J, Caillet H, Laplanche A, Boige V, Ducreux M, Duvillard P, Elias D, Schlumberger M, Sigal R, Baudin E. Detection of liver metastases from endocrine tumors: a prospective comparison of somatostatin receptor scintigraphy, computed tomography, and magnetic resonance imaging. *J Clin Oncol* 2005; **23**: 70-78 [PMID: 15625361 DOI: 10.1200/JCO.2005.01.013]

67 **Waldmann J**, Fendrich V, Habbe N, Bartsch DK, Slater EP, Kann PH, Rothmund M, Langer P. Screening of patients with multiple endocrine neoplasia type 1 (MEN-1): a critical analysis of its value. *World J Surg* 2009; **33**: 1208-1218 [PMID: 19350320 DOI: 10.1007/s00268-009-9983-8]

68 **Sundin A**, Vullierme MP, Kaltsas G, Plöckinger U; Mallorca Consensus Conference participants; European

Neuroendocrine Tumor Society. ENETS Consensus Guidelines for the Standards of Care in Neuroendocrine Tumors: radiological examinations. *Neuroendocrinology* 2009; **90**: 167-183 [PMID: 19077417 DOI: 10.1159/000184855]

69 **Wang Y**, Chen ZE, Yaghmai V, Nikolaidis P, McCarthy RJ, Merrick L, Miller FH. Diffusion-weighted MR imaging in pancreatic endocrine tumors correlated with histopathologic characteristics. *J Magn Reson Imaging* 2011; **33**: 1071-1079 [PMID: 21509863 DOI: 10.1002/jmri.22541]

70 **Jang KM**, Kim SH, Lee SJ, Choi D. The value of gadoxetic acid-enhanced and diffusion-weighted MRI for prediction of grading of pancreatic neuroendocrine tumors. *Acta Radiol* 2014; **55**: 140-148 [PMID: 23897307 DOI: 10.1177/0284185113494982]

71 **Lotfalizadeh E**, Ronot M, Wagner M, Cros J, Couvelard A, Vullierme MP, Allaham W, Hentic O, Ruzniewski P, Vilgrain V. Prediction of pancreatic neuroendocrine tumour grade with MR imaging features: added value of diffusion-weighted imaging. *Eur Radiol* 2017; **27**: 1748-1759 [PMID: 27543074 DOI: 10.1007/s00330-016-4539-4]

72 **Parikh T**, Drew SJ, Lee VS, Wong S, Hecht EM, Babb JS, Taouli B. Focal liver lesion detection and characterization with diffusion-weighted MR imaging: comparison with standard breath-hold T2-weighted imaging. *Radiology* 2008; **246**: 812-822 [PMID: 18223123 DOI: 10.1148/radiol.2463070432]

73 **Soyer P**, Boudiaf M, Placé V, Sirol M, Pautrat K, Vignaud A, Staub F, Tiah D, Hamzi L, Duchat F, Fargeaudou Y, Pocard M. Preoperative detection of hepatic metastases: comparison of diffusion-weighted, T2-weighted fast spin echo and gadolinium-enhanced MR imaging using surgical and histopathologic findings as standard of reference. *Eur J Radiol* 2011; **80**: 245-252 [PMID: 20650588 DOI: 10.1016/j.ejrad.2010.06.027]

74 **d'Assignies G**, Fina P, Bruno O, Vullierme MP, Tubach F, Paradis V, Sauvanet A, Ruszniewski P, Vilgrain V. High sensitivity of diffusion-weighted MR imaging for the detection of liver metastases from neuroendocrine tumors: comparison with T2-weighted and dynamic gadolinium-enhanced MR imaging. *Radiology* 2013; **268**: 390-399 [PMID: 23533288 DOI: 10.1148/radiol.13121628]

75 **Besa C**, Ward S, Cui Y, Jajamovich G, Kim M, Taouli B. Neuroendocrine liver metastases: Value of apparent diffusion coefficient and enhancement ratios for characterization of histopathologic grade. *J Magn Reson Imaging* 2016; **44**: 1432-1441 [PMID: 27227756 DOI: 10.1002/jmri.25320]

76 **Pereira JA**, Rosado E, Bali M, Metens T, Chao SL. Pancreatic neuroendocrine tumors: correlation between histogram analysis of apparent diffusion coefficient maps and tumor grade. *Abdom Imaging* 2015; **40**: 3122-3128 [PMID: 26280127 DOI: 10.1007/s00261-015-0524-7]

77 **De Robertis R**, Maris B, Cardobi N, Tinazzi Martini P, Gobbo S, Capelli P, Ortolani S, Cingarlini S, Paiella S, Landoni L, Butturini G, Regi P, Scarpa A, Tortora G, D'Onofrio M. Can histogram analysis of MR images predict aggressiveness in pancreatic neuroendocrine tumors? *Eur Radiol* 2018; **28**: 2582-2591 [PMID: 29352378 DOI: 10.1007/s00330-017-5236-7]

78 **Le Bihan D**, Breton E, Lallemand D, Grenier P, Cabanis E, Laval-Jeantet M. MR imaging of intravoxel incoherent motions: application to diffusion and perfusion in neurologic disorders. *Radiology* 1986; **161**: 401-407 [PMID: 3763909 DOI: 10.1148/radiology.161.2.3763909]

79 **Katharina Ingenerf M**, Karim H, Fink N, Ilhan H, Ricke J, Treitl KM, Schmid-Tannwald C. Apparent diffusion coefficients (ADC) in response assessment of transarterial radioembolization (TARE) for liver metastases of neuroendocrine tumors (NET): a feasibility study. *Acta Radiol* 2021; 2841851211024004 [PMID: 34225464 DOI: 10.1177/02841851211024004]

80 **Hwang EJ**, Lee JM, Yoon JH, Kim JH, Han JK, Choi BI, Lee KB, Jang JY, Kim SW, Nickel MD, Kiefer B. Intravoxel incoherent motion diffusion-weighted imaging of pancreatic neuroendocrine tumors: prediction of the histologic grade using pure diffusion coefficient and tumor size. *Invest Radiol* 2014; **49**: 396-402 [PMID: 24500090 DOI: 10.1097/RLI.0000000000000028]

81 **Ma W**, Wei M, Han Z, Tang Y, Pan Q, Zhang G, Ren J, Huan Y, Li N. The added value of intravoxel incoherent motion diffusion weighted imaging parameters in differentiating high-grade pancreatic neuroendocrine neoplasms from pancreatic ductal adenocarcinoma. *Oncol Lett* 2019; **18**: 5448-5458 [PMID: 31612053 DOI: 10.3892/ol.2019.10863]

82 **Rosenkrantz AB**, Padhani AR, Chenevert TL, Koh DM, De Keyzer F, Taouli B, Le Bihan D. Body diffusion kurtosis imaging: Basic principles, applications, and considerations for clinical practice. *J Magn Reson Imaging* 2015; **42**: 1190-1202 [PMID: 26119267 DOI: 10.1002/jmri.24985]

83 **Shi YJ**, Zhu HT, Liu YL, Wei YY, Qin XB, Zhang XY, Li XT, Sun YS. Radiomics Analysis Based on Diffusion Kurtosis Imaging and T2 Weighted Imaging for Differentiation of Pancreatic Neuroendocrine Tumors From Solid Pseudopapillary Tumors. *Front Oncol* 2020; **10**: 1624 [PMID: 32974201 DOI: 10.3389/fonc.2020.01624]

84 **Kartalis N**, Manikis GC, Loizou L, Albiin N, Zöllner FG, Del Chiaro M, Marias K, Papanikolaou N. Diffusion-weighted MR imaging of pancreatic cancer: A comparison of mono-exponential, bi-exponential and non-Gaussian kurtosis models. *Eur J Radiol Open* 2016; **3**: 79-85 [PMID: 27957518 DOI: 10.1016/j.ejro.2016.04.002]

85 **Pasicz K**, Podgórska J, Jasieniak J, Fabiszewska E, Skrzyński W, Anysz-Grodzicka A, Cieszanowski A, Kukołowicz P, Grabska I. Optimal b-values for diffusion kurtosis imaging of the liver and pancreas in MR examinations. *Phys Med* 2019; **66**: 119-123 [PMID: 31600671 DOI: 10.1016/j.ejmp.2019.09.238]

86 **Steinkohl E**, Bertoli D, Hansen TM, Olesen SS, Drewes AM, Frøkjær JB. Practical and clinical applications of pancreatic magnetic resonance elastography: a systematic review. *Abdom Radiol (NY)* 2021; **46**: 4744-4764 [PMID: 34076721 DOI: 10.1007/s00261-021-03143-3]

87 **Shi Y**, Gao F, Li Y, Tao S, Yu B, Liu Z, Liu Y, Glaser KJ, Ehman RL, Guo Q. Differentiation of benign and malignant solid pancreatic masses using magnetic resonance elastography with spin-echo echo planar imaging and three-dimensional inversion reconstruction: a prospective study. *Eur Radiol* 2018; **28**: 936-945 [PMID: 28986646 DOI: 10.1007/s00330-017-5062-y]

88 **Madhuranthakam AJ**, Yuan Q, Pedrosa I. Quantitative Methods in Abdominal MRI: Perfusion Imaging. *Top Magn Reson Imaging* 2017; **26**: 251-258 [PMID: 29176470 DOI: 10.1097/RMR.0000000000000145]

89 **Tofts PS**, Brix G, Buckley DL, Evelhoch JL, Henderson E, Knopp MV, Larsson HB, Lee TY, Mayr NA, Parker GJ, Port RE, Taylor J, Weisskoff RM. Estimating kinetic parameters from dynamic contrast-enhanced T(1)-weighted MRI of a

diffusable tracer: standardized quantities and symbols. *J Magn Reson Imaging* 1999; **10**: 223-232 [PMID: 10508281 DOI: 10.1002/(sici)1522-2586(199909)10:3<223::aid-jmri2>3.0.co;2-s]

90 **Donati F**, Boraschi P, Cervelli R, Pacciardi F, Lombardo C, Boggi U, Falaschi F, Caramella D. 3 T MR perfusion of solid pancreatic lesions using dynamic contrast-enhanced DISCO sequence: Usefulness of qualitative and quantitative analyses in a pilot study. *Magn Reson Imaging* 2019; **59**: 105-113 [PMID: 30878601 DOI: 10.1016/j.mri.2019.03.001]

91 **Kim JH**, Lee JM, Park JH, Kim SC, Joo I, Han JK, Choi BI. Solid pancreatic lesions: characterization by using timing bolus dynamic contrast-enhanced MR imaging assessment--a preliminary study. *Radiology* 2013; **266**: 185-196 [PMID: 23192779 DOI: 10.1148/radiol.12120111]

92 **Huh J**, Choi Y, Woo DC, Seo N, Kim B, Lee CK, Kim IS, Nickel D, Kim KW. Feasibility of test-bolus DCE-MRI using CAIPIRINHA-VIBE for the evaluation of pancreatic malignancies. *Eur Radiol* 2016; **26**: 3949-3956 [PMID: 26809293 DOI: 10.1007/s00330-016-4209-6]

93 **Basu B**, Basu S. Correlating and Combining Genomic and Proteomic Assessment with In Vivo Molecular Functional Imaging: Will This Be the Future Roadmap for Personalized Cancer Management? *Cancer Biother Radiopharm* 2016; **31**: 75-84 [PMID: 27093341 DOI: 10.1089/cbr.2015.1922]

94 **Binderup T**, Knigge U, Loft A, Federspiel B, Kjaer A. 18F-fluorodeoxyglucose positron emission tomography predicts survival of patients with neuroendocrine tumors. *Clin Cancer Res* 2010; **16**: 978-985 [PMID: 20103666 DOI: 10.1158/1078-0432.CCR-09-1759]

95 **Zhang P**, Yu J, Li J, Shen L, Li N, Zhu H, Zhai S, Zhang Y, Yang Z, Lu M. Clinical and Prognostic Value of PET/CT Imaging with Combination of ^{68}Ga-DOTATATE and ^{18}F-FDG in Gastroenteropancreatic Neuroendocrine Neoplasms. *Contrast Media Mol Imaging* 2018; **2018**: 2340389 [PMID: 29681780 DOI: 10.1155/2018/2340389]

96 **Reubi JC**, Waser B. Concomitant expression of several peptide receptors in neuroendocrine tumours: molecular basis for in vivo multireceptor tumour targeting. *Eur J Nucl Med Mol Imaging* 2003; **30**: 781-793 [PMID: 12707737 DOI: 10.1007/s00259-003-1184-3]

97 **Antwi K**, Fani M, Heye T, Nicolas G, Rottenburger C, Kaul F, Merkle E, Zech CJ, Boll D, Vogt DR, Gloor B, Christ E, Wild D. Comparison of glucagon-like peptide-1 receptor (GLP-1R) PET/CT, SPECT/CT and 3T MRI for the localisation of occult insulinomas: evaluation of diagnostic accuracy in a prospective crossover imaging study. *Eur J Nucl Med Mol Imaging* 2018; **45**: 2318-2327 [PMID: 30054698 DOI: 10.1007/s00259-018-4101-5]

98 **Regazzo D**, Barbot M, Scaroni C, Albiger N, Occhi G. The pathogenic role of the GIP/GIPR axis in human endocrine tumors: emerging clinical mechanisms beyond diabetes. *Rev Endocr Metab Disord* 2020; **21**: 165-183 [PMID: 31933128 DOI: 10.1007/s11154-019-09536-6]

99 **Beiderwellen KJ**, Poeppel TD, Hartung-Knemeyer V, Buchbender C, Kuehl H, Bockisch A, Lauenstein TC. Simultaneous 68Ga-DOTATOC PET/MRI in patients with gastroenteropancreatic neuroendocrine tumors: initial results. *Invest Radiol* 2013; **48**: 273-279 [PMID: 23493121 DOI: 10.1097/RLI.0b013e3182871a7f]

100 **Hope TA**, Pampaloni MH, Nakakura E, VanBrocklin H, Slater J, Jivan S, Aparici CM, Yee J, Bergsland E. Simultaneous (68)Ga-DOTA-TOC PET/MRI with gadoxetate disodium in patients with neuroendocrine tumor. *Abdom Imaging* 2015; **40**: 1432-1440 [PMID: 25820755 DOI: 10.1007/s00261-015-0409-9]

101 **Gillies RJ**, Kinahan PE, Hricak H. Radiomics: Images Are More than Pictures, They Are Data. *Radiology* 2016; **278**: 563-577 [PMID: 26579733 DOI: 10.1148/radiol.2015151169]

102 **Lubner MG**, Smith AD, Sandrasegaran K, Sahani DV, Pickhardt PJ. CT Texture Analysis: Definitions, Applications, Biologic Correlates, and Challenges. *Radiographics* 2017; **37**: 1483-1503 [PMID: 28898189 DOI: 10.1148/rg.2017170056]

103 **Canellas R**, Burk KS, Parakh A, Sahani DV. Prediction of Pancreatic Neuroendocrine Tumor Grade Based on CT Features and Texture Analysis. *AJR Am J Roentgenol* 2018; **210**: 341-346 [PMID: 29140113 DOI: 10.2214/AJR.17.18417]

104 **Choi TW**, Kim JH, Yu MH, Park SJ, Han JK. Pancreatic neuroendocrine tumor: prediction of the tumor grade using CT findings and computerized texture analysis. *Acta Radiol* 2018; **59**: 383-392 [PMID: 28766979 DOI: 10.1177/0284185117725367]

105 **Guo C**, Zhuge X, Wang Z, Wang Q, Sun K, Feng Z, Chen X. Textural analysis on contrast-enhanced CT in pancreatic neuroendocrine neoplasms: association with WHO grade. *Abdom Radiol (NY)* 2019; **44**: 576-585 [PMID: 30182253 DOI: 10.1007/s00261-018-1763-1]

106 **Reinert CP**, Baumgartner K, Hepp T, Bitzer M, Horger M. Complementary role of computed tomography texture analysis for differentiation of pancreatic ductal adenocarcinoma from pancreatic neuroendocrine tumors in the portal-venous enhancement phase. *Abdom Radiol (NY)* 2020; **45**: 750-758 [PMID: 31953587 DOI: 10.1007/s00261-020-02406-9]

107 **Li X**, Zhu H, Qian X, Chen N, Lin X. MRI Texture Analysis for Differentiating Nonfunctional Pancreatic Neuroendocrine Neoplasms From Solid Pseudopapillary Neoplasms of the Pancreas. *Acad Radiol* 2020; **27**: 815-823 [PMID: 31444110 DOI: 10.1016/j.acra.2019.07.012]

108 **Shindo T**, Fukukura Y, Umanodan T, Takumi K, Hakamada H, Nakajo M, Umanodan A, Ideue J, Kamimura K, Yoshiura T. Histogram Analysis of Apparent Diffusion Coefficient in Differentiating Pancreatic Adenocarcinoma and Neuroendocrine Tumor. *Medicine (Baltimore)* 2016; **95**: e2574 [PMID: 26825900 DOI: 10.1097/MD.0000000000002574]

109 **Jordan MI**, Mitchell TM. Machine learning: Trends, perspectives, and prospects. *Science* 2015; **349**: 255-260 [PMID: 26185243 DOI: 10.1126/science.aaa8415]

110 **Briganti G**, Le Moine O. Artificial Intelligence in Medicine: Today and Tomorrow. *Front Med (Lausanne)* 2020; **7**: 27 [PMID: 32118012 DOI: 10.3389/fmed.2020.00027]

111 **Yasaka K**, Akai H, Abe O, Kiryu S. Deep Learning with Convolutional Neural Network for Differentiation of Liver Masses at Dynamic Contrast-enhanced CT: A Preliminary Study. *Radiology* 2018; **286**: 887-896 [PMID: 29059036 DOI: 10.1148/radiol.2017170706]

112 **Luo Y**, Chen X, Chen J, Song C, Shen J, Xiao H, Chen M, Li ZP, Huang B, Feng ST. Preoperative Prediction of Pancreatic Neuroendocrine Neoplasms Grading Based on Enhanced Computed Tomography Imaging: Validation of Deep Learning with a Convolutional Neural Network. *Neuroendocrinology* 2020; **110**: 338-350 [PMID: 31525737 DOI:

10.1159/000503291]

113 **Zhou RQ**, Ji HC, Liu Q, Zhu CY, Liu R. Leveraging machine learning techniques for predicting pancreatic neuroendocrine tumor grades using biochemical and tumor markers. *World J Clin Cases* 2019; **7**: 1611-1622 [PMID: 31367620 DOI: 10.12998/wjcc.v7.i13.1611]

114 **Gao X**, Wang X. Deep learning for World Health Organization grades of pancreatic neuroendocrine tumors on contrast-enhanced magnetic resonance images: a preliminary study. *Int J Comput Assist Radiol Surg* 2019; **14**: 1981-1991 [PMID: 31555998 DOI: 10.1007/s11548-019-02070-5]

Published by **Baishideng Publishing Group Inc**
7041 Koll Center Parkway, Suite 160, Pleasanton, CA 94566, USA
Telephone: +1-925-3991568
E-mail: bpgoffice@wjgnet.com
Help Desk: https://www.f6publishing.com/helpdesk
https://www.wjgnet.com